ALPHA FOUNDATION FOR THE IMPROVEMENT OF MINE SAFETY AND HEALTH

Final Technical Report

Project Title	Further Characterizing Respirable Coal Mine Particulates: Submicron Particles, Metals and Diesel Exhaust
Grant Number	AFC316-17
Organization	Virginia Polytechnic Institute and State University
Principle Investigator	Emily Sarver 108A Holden Hall 445 Old Turner Street Blacksburg, VA 24061 Email: esarver@vt.edu Phone: 540-231-8139 Fax: 540-231-4070
Period of Performance	January 1, 2017-April 30, 2018

Acknowledgement/Disclaimer: This study was sponsored by the Alpha Foundation for the Improvement of Mine Safety and Health, Inc. (ALPHA FOUNDATION). The views, opinions and recommendations expressed herein are solely those of the authors and do not imply any endorsement by the ALPHA FOUNDATION, its Directors and staff.

Table of Contents

List of Figures

List of Tables

1.0 Executive Summary

Problem statement. Despite many decades of efforts aimed at understanding and reducing occupational lung disease amongst coal miners, incidence rates ticked up in the mid 1990s – and the most recent case reports indicate an alarming new era in very severe and rapidly progressive disease. The geographic clustering of many cases has drawn attention to the central Appalachian coalfields, where thin-seam mining is considered a key factor in disease risk. This is because thin-seam mining necessitates cutting significant rock along with the coal, and that rock can often contain crystalline silica, which has long been associated with severe interstitial lung disease. However, whether or not silica exposures are the only culprit in this new era of disease remains unclear. At least one reason for the uncertainty is that much is still not known about characteristics of respirable particulates in underground mines.

Prior work by our research team on another Alpha Foundation-funded project (AFC113-11) sought to begin filling in the knowledge gap on respirable coal mine dust characteristics. There, we used scanning electron microscopy with energy dispersive X-ray (SEM-EDX) to investigate the distribution of particles in dust samples from eight Appalachian coal mines. That work yielded important information about the primary types particles in the respirable dust fraction, and their likely sources. But it was limited to the supramicron range (i.e., > 1 μm), where most of the total dust mass is expected to occur. During our work though, we noted that submicron particles frequently occurred in very high numbers, and could sometimes be associated with diesel particulates or metals. As submicron particles and metals have not been widely explored in coal mine dusts, and diesel particulates are not generally measured due to analytical interferences with coal itself, the aim of our work here was to explore these constituents in order to expand the current understanding of respirable coal mine dust characteristics.

Research approach. For this work, we were able to leverage mine dust samples that had been collected on the previous project but not destructed. A total of 76 sample sets were available, each representing a unique sampling event (i.e., in a specific location within a specific mine). Samples from each set were analyzed to gather the following types of data: (1) the relative distribution of particles falling into a particular size bin (i.e., ultrafine = 100-400 nm, larger = 400-10,000 nm) and mineralogy class (i.e., carbonaceous, which generally include coal and diesel particulates; alumino-silicates or quartz, generally associated with dust produced from rock strata; carbonates, generally associated with application of rock dusting products; heavy minerals, which may be associated with multiple sources); (2) the mass concentrations of potentially bioaccessible and total acid-soluble metals and trace elements (i.e., Mg, Al, Si, K, V, Cr, Fe, Mn, Co, Ni, Cu, Zn, As, Se, Sn, Sr, Ag, Cd, Ba, Pb, U); and (3) the total mass concentration of commonly measured polyaromatic hydrocarbons (PAHs), which can be indicative of diesel exhaust, and the concentration of 1-nitroypyrene (1-NP), which has been suggested as a surrogate analyte for diesel exhaust. Following collection of these data, statistical analyses were conducted to determine whether significant differences could be identified between dust characteristics from particular mines or sampling locations, and whether significant correlations exist between particular dust variables.

Key findings. Notably: (1) Results supported the notion that there are four major types of particles in the coal mines represented here (i.e., coal dust, from the coal strata; mineral dust particles, from the rock strata being drilled or cut in the mine; mineral dust particles, generally carbonates, from rock dusting products; and diesel particulates). (2) Submicron particles generally account for >75% of total dust particles, and ultrafines generally account for >50%. (3) While diesel particulates appear to make up the largest fraction of ultrafines, mineral dusts (from rock strata and rock dust products) also frequently occur in this range. (4) Statistically significant differences were found between the mean particle size and mineralogy distributions observed for particular mines or sampling locations, but this was generally not true when comparing mean mine or location values for elemental concentrations, 1-NP or total PAHs. (5) However, significant correlations were found between many of the specific dust variables, including rock-strata sourced particles and certain metals and trace element; 1-NP and other variables presumed to be associated with diesel particulates (e.g., ultrafine carbonaceous particles and total PAHs); and rock-dust-product sourced particles and certain trace elements.

Impact. The results and analysis presented here provide new and more complete information about the range of possible respiratory exposures in coal mines. Such information is key for furthering both epidemiological and medical studies, and for development of more robust health surveillance programs. Moreover, project findings should inform mining professionals and researchers interested in development of more effective environmental monitoring programs and/or respirable particulate prevention or mitigation strategies.

2.0 Problem Statement and Objectives

Despite decades of efforts aimed at understanding and reducing occupational lung disease amongst coal miners, much is still unknown about characteristics of respirable particulates in underground mines. This is largely because dust exposures in mines are regulated, and thus usually studied, using just two metrics: the total mass concentration of respirable dust, and the mass fraction of quartz (i.e., crystalline silica) in that dust.

While measuring and targeting reductions in these metrics undoubtedly led to dramatic improvements and declining disease rates over several decades, these rates have more recently stalled or even appear to be reversing in some regions [e.g., Antao et al., 2005; Attfield and Sexias, 1995; Suarthana et al., 2011; Gibson, 2016; Zosky et al., 2016]. **Over the past few years, an alarming number of cases have been diagnosed in central Appalachia, in particular, many of which appear to be rapidly progressive forms of disease [e.g., Gamble et al., 2011; Blackley et al., 2014, 2016 and 2018]. This observation has yet to be conclusively explained, but contributing factors could certainly include specific dust characteristics (e.g., certain mineral or organic constituents, particularly small particles).**

On a prior project funded by the Alpha Foundation (AFC113-11), we began exploring the whole composition of respirable coal mine dust. Using a computer controlled routine on a scanning electron microscope with energy dispersive x-ray (CC-SEM-EDX), we specifically determined the mineralogical (number) distribution of supramicron particles (i.e., > 1 μm) collected from eight mines across central and northern Appalachia [Johann-Essex et al., 2017a and 2017b]. Our results indicated that, in addition to coal, most respirable dust samples contained significant abundances of mineral particles, which were attributed to either cutting/drilling of rock strata in the mine or application of rock dusting products (i.e., to mitigate explosibility hazards). While that work was limited to quantifying particles in the supramicron range, in our efforts to establish and verify the CC-SEM-EDX routine, we observed that most samples also contained many submicron particles (i.e., < 1 μm). We also occasionally observed particles that contained heavy minerals and particles that resembled diesel particulate matter (DPM) based on their morphology.

Although minor dust constituents and submicron particles, in general, may contribute relatively little to the total respirable dust mass, they may be important for gaining a more complete picture of dust exposures, and their possible health implications. The following section provides an overview on submicron particles, metallic and trace constituents in dust, and diesel exhaust (DE).

2.1 Background

2.1.1 Submicron Particles

Broadly, exposure to submicron airborne particulates is increasingly considered a concern for human health. Such particles can penetrate deeper into the alveoli and are not cleared as efficiently as larger particles; have increased mobility within the respiratory system, or beyond via translocation to blood; have increased reactivity with lung tissue related to their increased surface area or altered morphology; and can present co-exposure risks as they combine with other particles and either enhance the intake rate of or physiological response to one another [Langrish et al. 2011; Oberdörster et al. 2005]. Due to their size, submicron particles are also difficult to abate [McKenna, 2008] and can remain suspended in the air indefinitely – particularly in environments

with relatively high airflow rates, like underground mines which must employ significant ventilation.

Though submicron particles have gained a lot of attention, particularly in the context of public health and ambient exposures [e.g., see Niu et al., 2010; Cabada et al., 2004; Donaldson et al., 1998], very little is known about the relative occurrence or implications of submicron particles in coal mine environments. It is well established that the proportion of fine particles (e.g., less than about 75μm) in airborne coal mine dust is much higher now than it was decades ago [Sapko et al., 2007] – likely due to more powerful cutting machines – but the proportion of respirable, let alone submicron, particles has not been well documented. Likewise, health effects in miners have not been reported as a function of particle size. Some recent basic research on crystalline silica, which is widely considered the most harmful constituent of respirable mine dusts, concluded that submicron silica particles (geometric mean size of 0.3μm) can accelerate detrimental macrophage responses in lung tissue versus larger respirable particles (geometric mean size of 4.1μm) [Mischler et al., 2016].

While determining the relative mass concentration of total submicron versus total respirable dust can be done quite simply using different size selectors for sampling, dust particle characterization is fairly challenging. As mentioned above, SEM-EDX represents one option for such work, as it can resolve particle size, morphology, and elemental composition [Mitsche et al., 2006; Hartman et al., 2012]. It has been used characterize various types of particulates including street dust, indoor aerosols, fly ash, and lab generated dust samples, even in the submicron range [e.g., Fedotov et al., 2014; Zamengo et al., 2009; Poelt et al., 2002; Brunner et al., 2000; Kaufherr and Lichtman, 1984]. However, due to the fact that SEM-EDX analysis is very time and cost intensive, it has not been commonly used on mine dusts. To our knowledge, our own work on supramicron particles from eight mines (i.e., Johann-Essex et al., 2017b) represents the most comprehensive work to date to do particle-level characterization of respirable dust in coal mines. Although this work used a CCSEM-EDX routine, our experience has shown that analysis in the submicron range is also possible, at least using manual SEM-EDX.

2.1.2 Metals and Trace Constituents

Trace constituents in respirable particulates can include metals (e.g., Fe, Al, Co, Ni, Pb) and other inorganic elements (e.g., Se, As), as well as bound organic compounds such as polyaromatic hydrocarbons (PAHs) [Pandey et al., 2013]. While exposures to atmospheric particulate matter, in general, has long been recognized as a health hazard, interest has been steadily growing in understanding the specific characteristics that represent the most significant toxicity risks; and a wealth of literature is now available on the topic of trace constituents and associated risks [Li et al., 2015]. However, there has been almost no research on trace constituents in respirable coal mine dust. Based on detailed studies of raw coal, it is widely known that trace elements (e.g., Ba, As, Cr, Se, Ni, Pb, V) are commonly associated with both the organic (i.e., coal) and mineral matter (i.e., "ash"), especially when pyrite and clay minerals are present [Maiti and Mishra, 2013; Aneja et al., 2012; Dubey et al., 2012; Sharkey et al., 1975]. However, whether or not these elements are substantially contained in the respirable fraction of dust generated during mining and auxiliary activities is unknown.

A limited amount of research has been conducted surrounding reactive metallic minerals in coal and potential health outcomes. Correlations between coal mineralogy and epidemiological data have suggested that bioavailable Fe, for example, may play a role in development of CWP [Huang et al., 2013; Harrington et al., 2012; Dalal et al., 1995; Ghio and Quigley, 1994; Guest, 1978], especially if the coal has high pyrite content [Cohn et al., 2006]. But to our knowledge, bioavailable Fe (or other metals) in respirable particulates from coal mine environments have not actually been measured; thus the suggested exposure pathway has not been proven.

With regard to quantifying metals and trace elements in airborne particulates, methods typically include digestion of the particles followed by analysis of the digestate (e.g., by inductively couple plasma with mass spectrometry, ICP-MS) to determine mass concentrations (e.g., mg/g) [e.g., see Pan et al., 2015, Niu et al., 2010; Furuta et al., 2005; Samara and Voutsa, 2005]. Strong acid solutions can be used for the digestion to determine total extractable concentrations. For estimating potentially bioavailable concentrations, the digestion can be done in simulated lung fluid (SLF) [Pelfrêne et al., 2017; Kastury et al., 2017; Dean et al., 2017; Julien et al., 2011].

In addition to inorganic trace constituents in respirable coal mine particulates, there may be organic trace constituents such as PAHs. These compounds have been long been recognized as hazardous air pollutants, with a variety of health effects [ATSDR, 1995]. PAHs are known to be sourced from both raw coal and combustion of coal and other fossil fuels, including diesel, and can exist as solids themselves or be sorbed to particulates [Kim et al., 2013; ATSDR, 1995]. Analysis of PAHs in particulate samples is well established using solvent extractions followed by gas (GC-MS) or liquid chromatography with mass spectrometry (LC-MS) [e.g., Shang et al., 2014]. While several studies have evaluated PAH concentrations associated with unburnt coal particles in ambient environments [e.g., see Liu et al., 2012; Achten and Hofman, 2009], again we find no literature to suggest that PAHs have been measured in underground coal mine environments.

2.1.3 Diesel Exhaust

DE represents another airborne contaminant that has not been well characterized in coal mines. In occupational environments, DE exposures are often monitored by monitoring DPM, which is the solid portion of DE. DPM itself is a complex and heterogeneous mixture of many constituents. It is associated with a variety of acute and chronic health risks [WHO, 2012] and is known to occur primarily in the submicron size range as single particles or agglomerates [Bugarski et al., 2011]. In metal/non-metal mines in the US, personal DPM exposures are monitored using total carbon (TC) as a surrogate analyte [MSHA, 2006]; in coal mines, however, coal particles themselves present obvious analytical interferences [Schauer, 2003]. So, at present, DPM is only measured at the tailpipe of regulated equipment in US coal mines [MSHA, 2001], which limits understanding of personal exposures or concentration at any particular location to very rough estimates.

To allow for monitoring of personal exposures to DE/DPM where TC interferences exist, the chemical 1-nitropyrene (1-NP) has been suggested as an alternative surrogate analyte [Scheepers et al., 2003; Talaska et al., 1996; Scheepers et al., 1995]. 1-NP is a nitrated PAH, which is preferentially formed by the specific high-temperature combustion processes in a diesel engine. It is relatively abundant in DE and is known to efficiently sorb to the solid DPM [Bezabeh et al., 2003; Gallagher et al., 1994; Scheepers and Bos, 1992]. Moreover, 1-NP has not been detected in significant levels in coal dust, coke oven emissions, bitumen fumes or cigarette smoke, such that

these sources would not confound its association with DPM exposure. To date, only one study has investigated 1-NP in an underground coal mine operating diesel equipment [Scheepers et al., 2003], but results were promising in that the chemical could be quantified and correlated with DE.

Incidentally, DE/DPM may contain a range of other PAHs in addition to 1-NP [Bugarski et al., 2011]. As mentioned above, these chemicals have generally not been studied in coal mines. Given that analytical methods are relatively similar for most PAHs, coupling efforts to determine 1-NP and other PAHs may be an efficient approach to further characterizing respirable mine particulates.

2.2 Research Aim and Objectives

Building on our prior findings from project AFC113-11, and directly aligned with the Foundation's *Disease Exposure and Risk Factors* focus area, **the specific aim of this project was to expand the current understanding of respirable coal mine dust characteristics**. For this, we were able to use the same collection of Appalachian dust samples from the earlier work and we sought characterize them based on: compositional distribution of submicron particles, with comparison to the distribution of supramicron particles (Objective 1); mass concentrations of potentially bioavailable metals and trace elements (Objective 2); and mass concentrations of PAHs including 1-nitropyrene (1-NP), which has been specifically associated with diesel exhaust (Objective 3). It is noted that a few studies have touched separately on these metrics in the context of coal mine dust [e.g., Riley et al. 2018; Birch and Noll, 2004; Huang et al., 2006; Scheepers et al., 2003], but none have been widely investigated – and this effort represents the first known attempt to so fully characterize respirable coal mine dust. Further, to understand variability in dust characteristics and gain insight to likely dust sources, all results were analyzed to determine whether specific characteristics are correlated to one another, particular mines or sampling locations (Objective 4).

3.0 Research Approach

As part of the previous AFC113-11 project work, our team gathered a large collection of respirable dust samples from eight underground coal mines in three distinct regions of Appalachia (Figure 1). These samples were collected between July 2014 and July 2015, and a description of mine characteristics at the time of sampling is provided in Table 1. All samples were collected in "sets", meaning multiple samples were collected simultaneously in a particular location in the mine. While some samples in each set were destructed for analysis on the previous project, others were not and were thus available for further analysis on the current project. The following sections describe the dust samples and analytical methods used here.

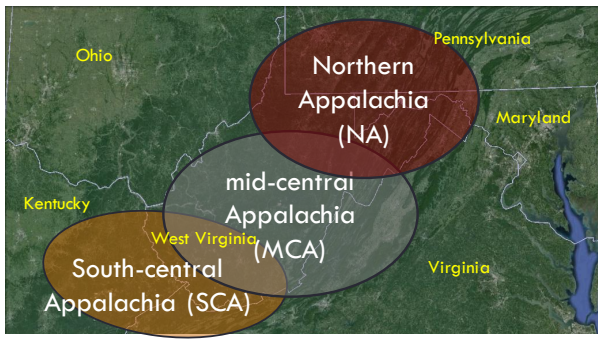

Figure 1. Three mine regions where respirable coal mine dust samples were collected.

Table 1. General characteristics of mines where dust samples were collected for this project [modified from Johann-Essex et al., 2017a].

	MCA				NA		SCA	
Characteristics	**Mine 1**	**Mine 2**	**Mine 3**	**Mine 4**	**Mine 5**	**Mine 6**	**Mine 7**	**Mine 8**
Primary coal seam	Eagle	Powellton	Peerless	Cedar Grove	Pittsburgh #8	#2 Gas	Alma	Alma
Seam thickness (ft)	3-5	3-4	4.5	2-4	6-8	6.5	5-6	4-4.5
Total mining height (ft)	5	5.5	6	4	8	8	6-7	6
Primary rock strata	sandstone	sandstone	shale and sandstone	sandstone	sandy shale and slate	shale	sandy shale and slate	shale
Number of sections	2 CM	2 CM	2 CM	2 CM	1 LW; 3 CM	1 LW; 5 CM	3 CM	2 CM
Production (10^6 tons/yr)	0.45	0.45	0.84	0.55	2.4	7.5	1.3	0.9
Typical dust conc.[1]	low to moderate	low to moderate	low to moderate	low	low to high	low to moderate	low to moderate	low to moderate
Typical quartz percentage[2]	low to moderate	low to high	low to moderate	low to high	low	low	low to moderate	low to high

[1]based on operator and inspector mine samples collected between 2013-2016; low = <0.6 mg/m^3, moderate = 0.6-1.8 mg/m^3, high = >1.8 mg/m^3

[2]based on operator and inspector mine samples collected between 2013-2016; low = <5.0%, moderate = 5.0-9.0%, high = >9.0%

3.1 Description of Dust Samples

All dust samples were collected by our research team using Escort ELF pumps (set to 1.7 LPM flowrate) and Dorr-Oliver cyclones. These are the same equipment used to collect respirable dust samples in coal mines for compliance monitoring (i.e., for post-collection gravimetric and crystalline silica analyses). The cyclone removes oversized particles such only those in the

respirable range (i.e., < 10 µm) are deposited on the sample filter. At 1.7 LPM, the cyclone produces a d_{50} cut size of about 4 µm. Samples were collected onto various filter media (37-mm diameter) housed within two-piece styrene cassettes. Those collected onto polycarbonate (PC) filters were not previously destructed and were available for the current project.

In each mine, samples were collected in five general locations, which are described below. These were chosen to represent distinct environments with respect to potential dust sources.

- Intake (I): samples collected in intake airways just outby of the primary production area (including the headgate of a longwall section) and samples collected near the mantrip track
- Feeder (F): samples collected near the feeder breaker or along the main conveyor belt
- Production (P): samples collected near continuous miner machines or the midface of a longwall section
- Roof bolter (B): samples collected just downwind of an active roof bolter
- Return (R): samples collected in the return airway just outby of the primary production area (including the tailgate of a longwall section), and samples collected near active trickle duster machines in return airways.

In total, there were 76 unique sampling events (i.e., sample collection in a particular location of a particular mine), during which a set of multiple samples were collected simultaneously and side-by-side, such that they can be considered replicates. Each set included at least two samples collected onto PC filters. These filters are appropriate for analysis by SEM-EDX due to their smooth surface and homogeneous pore size (0.4 µm). For the previous project, a 9-mm subsample was removed from the center of each PC filter in order to characterize supramicron particles by CCSEM-EDX [Johann-Essex et al., 2017a and 2017b]. For the current project, one of the subsamples from each sample set was re-analyzed using manual SEM-EDX to characterize submicron particles (Figure 2). Then, then remnant of the filter from which that subsample had been taken was analyzed to determine mass concentrations of metals and trace elements; and, for some sample sets, the remnant of a replicate filter was also analyzed to determine concentrations of 1-NP and PAHs.

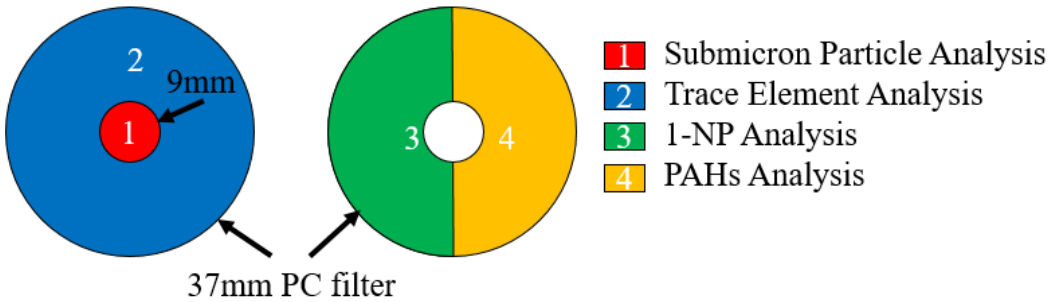

Figure 2. Areas of replicate filter samples used for various analysis. On the subsample (i.e., red area "1") used for submicron particle analysis here, supramicron particle analysis had already been completed on the previous AFC113-11 project.

Table 2 shows by mine and sampling location the number of samples included in each type of analysis. For submicron particle characterization, a total of 76 samples were analyzed (i.e., one for each unique sample set). For metals and trace elements analysis, only 74 samples were analyzed, as significant mass loss occurred during preparation of two samples. A total of 37 samples were selected for 1-NP and PAHs analysis. These included all available samples from Mine 4 (i.e., a

total of eight samples from four sample sets, each with two replicates) and Mine 6 (i.e., a total of 14 samples from 14 sets, each with one replicate), which were known to operate diesel equipment during the sample collection. Another 15 total samples were also selected from the other mines, and represented a various sampling locations. Significant mass loss also occurred during preparation of one sample for 1-NP analysis, such that only 36 samples were analyzed for 1-NP. Table 2 also shows the number of results used in correlational analysis, which is discussed later.

Table 2. Number of samples analyzed for submicron particles (S), metals and trace elements (M), and 1-NP and PAHs (P) by mine and sampling location. The table also shows the number of results used for correlational analysis between S and M metrics, and between S, M and P metrics.

Region and Mine		Sampling Location and Dust Analysis															Total Samples Analyzed			Results for Correlation Analysis	
		B			F			I			P			R							
		S	M	P	S	M	P	S	M	P	S	M	P	S	M	P	S	M	P	S/M	S/M/P
MCA	Mine 1	3	3	1	1	1	0	1	1	0	1	1	1	1	1	0	7	7	2	7	2
	Mine 2	2	2	0	1	1	1	1	1(0)[1]	1[2]	1	1	1	1	1	0	6	5	3	5	2
	Mine 3	1	1	1	1	1	1	1	1	0	1	1	0	1	1	0	5	5	2	5	2
	Mine 4	1	1	2[3]	1	1	2[3]	1	1	2[3]	0	0	0	1	1	2[3]	4	4	8	4	4
NA	Mine 5	1	1	0	3	3(2)[1]	2	2	2	0	1	1	1	3	3	1	10	9	4	9	3
	Mine 6	1	1	1	3	3	3	6	6	5[4]	1	1	1	4	4	4	15	15	14	15	14
SCA	Mine 7	2	2	0	3	3	0	2	2	0	4	4	1	3	3	1	14	14	2	14	2
	Mine 8	2	2	0	3	3	1	3	3	0	3	3	1	4	4	0	15	15	2	15	2
Total		13	13	5	16	15	10	17	16	8	12	12	6	18	18	8	76	74	37	74	31

[1] Sample loss during preparation for metals analysis; value in parenthesis indicates the number of samples for which results were obtained

[2] Sample not included in correlational analysis since no corresponding metals results were available

[3] These two samples were collected as duplicates and their results were averaged for use in correlational analysis since corresponding metals results were only available from one sample

[4] Sample loss during preparation for 1-NP analysis, but PAH analysis was completed

3.1 Characterization of Submicron Particles

On each of the 76 samples mentioned above, submicron particles were analyzed by our research team using SEM-EDX.[1] All work was done manually using an FEI Quanta 600 FEG environmental SEM (FEI, Hillsboro, OR) equipped with a Bruker Quantax 400 EDX spectroscope (Bruker, Ewing, NJ). The EDX was operated in backscatter mode, and Bruker's Esprit software (Version 1.9) was used to collect elemental spectra on each particle selected for analysis. This is the same instrument and software that were used during the prior project (AFC113-11) to analyze supramicron particles on the same samples. For comparison, Table 3 highlights the key differences between the submicron analysis conducted here and the supramicron analysis done earlier.

Since the objective of SEM-EDX work was to characterize compositional (i.e., mineralogic) distributions of particles in each sample, it was important to select and analyze particles across a

[1] Consistent with the original project proposal, we did investigate the feasibility of using a CCSEM-EDX routine, similar to the one we developed for supramicron particle analysis on the previous project [see Johann-Essex et al., 2017a]. However, we quickly came to the conclusion that two primary challenges could not be overcome within the current project timeframe. First, the automation software we are using has a tendency to mistake filter pore edges as particles. Second, the filter background causes significant interference with EDX results at the higher magnification required for analyzing submicron particles. This means that compositional classification criteria may need to be tweaked often during analysis.

wide area of each sample in order to ensure that results are representative. Previous work in the supramicron range indicated that analysis of 100 particles per sample was likely sufficient in the supramicron range (Sellaro et al., 2015), and analysis of 500 particles produced statistically reproducible results (Johann-Essex et al., 2017a). Based on preliminary work on the current project, we decided that a target of 250-300 total submicron particles per sample was optimal with respect to gathering robust data while limiting analysis time to about 4 hours per sample.

Table 3. Description of sub- and supramicron particle analysis by SEM-EDX.

Parameter	**Submicron Analysis**	**Supramicron Analysis**
Method	Manual	Computer Controlled
Magnification	20000X	1000X
Spot size	4	6.5
Voltage (kV)	10	15
Working distance (mm)	12.5	12.5
Frames/sample (range)	17-189	10-157
Frames/sample (average)	69	33
Particle/frame	7	50
Particle/sample (range)	83-315	61-500
Particle/sample (average)	236	489
Mineralogy classes	Carbonaceous (coal and DPM), Alumino-silicates, Quartz, Carbonate, Heavy Mineral, Other (includes other minerals)	Carbonaceous (only coal), Alumino-silicates, Quartz, Carbonate, Heavy Mineral, Other (any particle that does not fit into the defined classes above)
Cross-sectional diameter (µm)	0.1-1	1-10

A detailed description of the manual SEM-EDX routine used here, including the method used to select individual particles for analysis, is provided in Appendix A. Briefly, two primary types of data were collected for each particle: long and intermediate dimensions[2] for sizing, and EDX spectral peaks for classifying mineralogy. As for our previous work on supramicron particles, classification criteria for the submicron particles were developed and verified using high-purity materials (Table 4). These materials were chosen to represent the major mineralogic categories for particles typically found in coal mine dust.

Table 4. Minimum spectral peak heights (in cps/eV) determined for submicron particles from pure and known materials. These serve as the basis for mineralogic classification criteria for manual SEM-EDX analysis.

Material	**C**	**Al**	**Si**	**Ca**
Calcite	-	-	-	≥0.3
Quartz	-	-	≥0.2	-
Kaolinite	-	≥0.5	≥0.5	-
Coal	≥45	-	-	-
Shale	-	≥1	≥1	-
Rock Dust	-	-	-	≥0.3

[2] The long dimension is defined as the particle length at its widest point in the plane of view under the SEM, and the intermediate dimension is defined as the length that is perpendicular to long.

Using the classification criteria, a total of five mineralogy classes were defined: carbonaceous (C), alumino-silicate (AS), quartz (Q), carbonate (CB), and heavy mineral (HM). Particles that do not fit into one of these categories based on their EDX spectra were classified as "other" (O). It is important to note that the C category can include both coal and DPM particles in the submicron range, whereas this category is generally believed to include only coal particles in the supramicron range. As shown in Figure 3, DPM can be distinguished from coal in some cases by its characteristic morphology (i.e., aggregated chains of nano-sized carbon spheres). However, the image resolution at the standard 20,000x magnification used for submicron SEM-EDX work here does not always allow for this distinction.

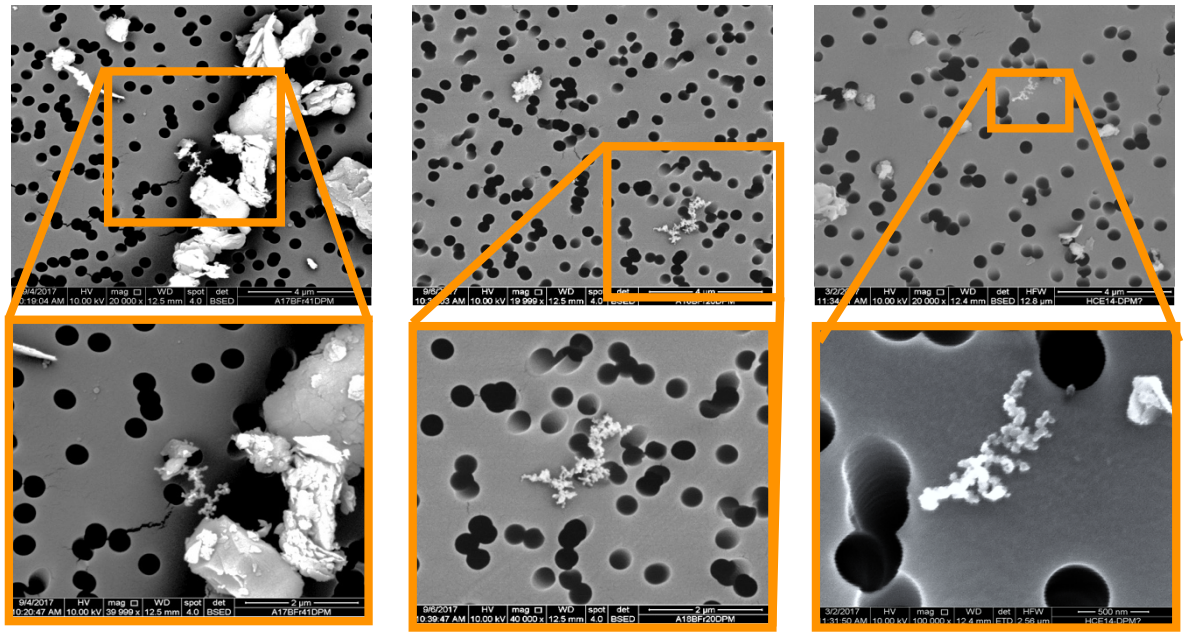

Figure 3. Examples of DPM particles in dust samples from several mines. In some cases, DPM can be identified by its characteristic morphology of chains or clusters of nano-sized carbon spheres. Images in the upper panel were collected at the 20,000x standard magnification used for the manual SEM-EDX work to characterize submicron particles. Images in the lower panel were collected at 40,000x (left and middle) and 100,000x (right).

Using mineralogic classification and size data, submicron particle distributions were computed for each sample; and supramicron distributions were already computed on the previous project (AFC131-11). To merge the two datasets, particle counts were normalized on a unit-area basis to determine an effective particle density (#/μm^2) in both size ranges. For the submicron particles, densities were estimated during the manual SEM-EDX work by gathering analyzed-area data in real time. For supramicron particle density estimation, we had to use the SEM images collected on the prior project. From these, we could assess how much total area of the sample filter was analyzed to complete the analysis (i.e., on 500 total particles per sample). Using the relative particle densities in the sub- and supramicron ranges, distributions across the entire 0.1-10 µm (100-10,000 nm) range could be estimated. For data analysis, three discreet bins were set to cover what we operationally defined as ultrafine (100-400 nm) and fine (400-1,000 nm) particles in the submicron range, and larger particles in the supramicron range (1,000 nm – 10,000 nm).

3.2 Determination of Metals and Trace Element Concentrations

Analysis for metals and trace elements was completed on 74 mine samples as shown in Table 2. Following removal of the 9-mm subsample from each filter that was used for SEM-EDX analysis (see Figure 2), the rest of the filter had been kept in its original cassette until it was prepared for the metals and trace elements analyses. Prior to work with the mine samples, the analytical method used here was tested on a total of 50 lab-generated respirable dust samples, which were collected by aerosolizing several known source materials (i.e., clean coal from high- and low-pyrite seams, and high-ash raw coal). This work allowed our research team to gain valuable experience in sample preparation techniques necessary for working with very small samples (i.e., sometimes just 10 µg or less), as well as insights into the possible wide variability in elemental concentrations in different dust materials.

The analytical method used here was modified to determine mass concentrations of potentially bioavailable and total acid-soluble metals and trace elements in respirable coal mine dust samples. The method includes two sequential digestions, and a detailed description is provided in Appendix B. Briefly, dust was removed from each PC filter in ultra-pure water (i.e., 18 MΩ) under sonication, and then centrifuged. The total dust mass recovered was determined gravimetrically by weighing the dry filter before and after dust removal. The recovered dust was dried and then exposed to SLF, which was prepared using a recipe published by Pelfrêne et al. (2017). The digestate solution was filtered to collected un-dissolved dust particles and collected for analysis of metals and trace elements by ICP-MS using a Thermo Electron X Series instrument (Thermo Fisher Scientific, Waltham, MA). The remaining dust was then exposed to a strong acid solution (per ASTM D7439-14), which was again filtered and collected for ICP-MS analysis. The following elements were included in the ICP-MS analysis and are reported here: Mg, Al, Si, K, V, Cr, Fe, Mn, Co, Ni, Cu, Zn, As, Se, Sn, Sr, Ag, Cd, Ba, Pb, U.[3] Minimum reporting levels and detection limits are discussed in Appendix B.

Elemental masses measured in the SLF digestate were used to determine potentially bioaccessible concentrations of metals and trace elements on a dry dust mass basis (mg/g); and the sum of elemental masses measured in the SLF and strong acid digestates were used to determine total acid-soluble concentrations. In cases where the recovered dust mass was measured to be less than 2 µg, the mass was assumed to be 2 µg, which is the lower limit on readability for the microbalance used here (Sartorius CPA26P, Sartorius AG, Göttingen, Germany). This assumption was made to limit the tendency for very low mass samples to result in inordinately high elemental concentrations. Further, in instances where elemental concentrations were still found to be extraordinarily high (i.e., > 500 mg/g, meaning the element would constitute 50% of the total dust mass analyzed), the concentration as assumed to be 500 mg/g for data presentation and analysis.

3.3 Determination of 1-NP and PAH Concentrations

A total of 37 mine samples, representing 33 of the 76 available sample sets (per Table 2) were sent to the University of Washington (UW) for 1-NP and PAH analysis. An additional six lab-generated samples were also sent. These were made by aerosolizing pulverized clean or raw coal materials, and collecting the respirable particles onto PC filters (i.e., identical to those on which the mine

[3] Several elements (i.e., Na, Ca, Cl, S, P, Ti, Mo) are not reported due to significant interferences from the chemistry of the digestion solutions, or quality of the ICP-MS data. Further explanation is provided in Appendix B.

dust samples had been collected). The lab-generated samples were meant to provide some insight on possible 1-NP and PAH concentrations in particulates sourced only from coal materials (i.e., not containing DE/DPM).

To analyze the samples, UW modified their standard extraction procedures to be compatible with use for PC filter media, and otherwise generally followed published methods for measurement of 1-NP [Miller-Schulze et al., 2007] and PAHs [USEPA, 2007; Shang et al., 2014] in particulate samples. A brief description of the methods follows.

Sample filters were transferred to filters to glass vials and spiked with an internal standard mixture of deuterated 1-NP and 16 PAHs (Table 5). These are known as the "EPA PAHs" and are commonly used as indicator analytes for the broad category of PAHs, which includes numerous compounds. Following spiking with the internal standards, hexane was added to the sample vials as a solvent to extract the organic compounds, and they were sonicated for 30 minutes. Then, filters were removed from the hexane extract and an equal volume of dichloromethane was added to the hexane to promote further extraction, followed by an additional 30 minutes of sonication. The extracts were concentrated by evaporation under nitrogen at 50°C, filtered, and split into equal portions for the 1-NP and PAH analyses. Both portions were then evaporated to dryness. Samples were reconstituted in an ethanol-buffer mixture for 1-NP and toluene for PAHs. The lab-generated dust samples were extracted using a similar procedure as for the mine samples, but they were also centrifuged to remove the majority of the dust particles prior to filtering. Finally, the reconstituted samples were analyzed using a 2-dimensional high-performance LC with tandem MS assay (2D-HPLC-MS/MS) to determine mass of 1-NP and a GC-MS/MS assay to determine the masses of the 16 EPA PAHs.

Table 5. List of 16 EPA PAH compounds, along with molecular weights and number of benzene rings included in the compound structure.

Compound	Molecular Weight (g/mol)	Number of Rings
Naphthalene	128	2
Acenaphthylene	152	3
Acenaphthene	154	3
Fluorene	166	3
Phenanthrene	178	3
Anthracene	178	3
Pyrene	202	4
Fluoranthene	202	4
Chrysene	228	4
Benzo(a)anthracene	228	4
Benzo(b)fluoranthene	252	5
Benzo(a)pyrene	252	5
Benzo(k)fluoranthene	252	5
Benzo(g,h,i)perylene	276	6
Indeno[1,2,3-cd]pyrene	276	6
Dibenz(a,h)anthracene	278	6

HPLC work was performed using an Agilent 1100 HP liquid chromatograph with a 6410 tandem mass spectrometer (Agilent, Santa Clara, CA). Based on historical data in the UW laboratory, the instrument limit of detection for 1-NP is 0.2-2.7 pg per sample extract, and the accuracy and precision of the analysis is 87±7%. GC work was performed using an Agilent 7890B gas chromatograph coupled with a 7000 GC/MS triple quadrupole mass spectrometer. Based on the data of Shang et al. (2014), UW reported that the expected accuracy of the assay used here is between 75-126% and the limit of detection is 10 pg per injection (2 µL per sample). For the mine samples, it was observed that recoveries for internal standard compounds with molecular weights less than that of phenanthrene (see Table 5) were very low and variable, which increases uncertainty of the results. Thus, only results for the 12 EPA PAHs with molecular weights greater than or equal to phenanthrene were reported by UW. Further, given the relatively low mass values measured for most of the reported compounds, it was decided to sum all PAHs measured and reported for each sample to obtain total PAHs.

The analysis performed by UW resulted in 1-NP and PAH mass values per sample, but to determine mass *concentrations* (i.e., on a dry dust basis, µg/g), the dust mass recovered from the sample filter must be known. Since UW was not able to measure this quantity for the mine samples, the mass recovered on each corresponding (i.e., replicate) sample during the metals and trace elements analysis was therefore used as an estimate. It is noted that the UW researchers did visually observe dust loss on some samples (i.e., particles on the cassette walls and filter support pad), which may have occurred during shipment or handling. Regardless, this observation may mean that recovered dust masses were substantially different between replicate samples prepared for analysis by our team versus by UW – and results should be interpreted accordingly.

3.4 Data Analysis

Using the methods described in the above sections, a wealth of data was collected on the respirable mine dust samples available for this project. To determine whether significant differences could be observed between dust characteristics from particular mines or sampling locations, statistical analysis was performed to explore the following variables:

- Number percentage of total particles in the ultrafine size range (i.e., 100-400 nm, referred to from here as "ultrafine particles"), or in the fine and supramicron range, (i.e., 400-10,000 nm, referred to from here as "larger particles"). For these variables, n = 76 data points were available.
- Number percentage of ultrafine or larger particles in each defined mineralogical class (i.e., C, AS, Q, CB, and HM). For these variables, n = 76.
- Mass concentration (mg/g) of potentially bioaccessibility and total acid-soluble elements (i.e., Al, Si, K, Fe, Zn, Cr, Mn, Co, Ni, Cu, Ag, Ba). For these variables, n = 74.
- Mass concentration (µg/g) of 1-NP (n = 36) and the total PAHs (n = 37).

To perform the statistical analysis, Minitab 18 software was used (Minitab 18, 2018). First, normality of each data set (i.e., for each variable) was checked, and all sets were found to have normal or near-normal distributions. Each data set then was tested for equal variance using Levene's Test; this was to determine whether or not the variance or standard deviation of the data groups (i.e., mines or locations) are different. If variances were found to be equal, standard analysis of variance (ANOVA) testing was used to determine whether statistical differences exist between

group means (e.g., do number percentages of ultrafine particles vary by mine?); and, if so, Tukey Tests were used to identify where those differences occurred (e.g., ultrafine particle percentages were higher in Mine 6 than in Mine 5). In instances where data groups were found to have unequal variances, Welch's Test was used to determine whether statistical differences existed between the groups, and Games-Howell Tests were used to identify the differences. For all of these statistical analyses, a significance level of 0.05 (95% confidence interval) was considered.

In addition to efforts to determine whether dust characteristics varied by mine or sampling location, analysis was also conducted to determine whether correlations exist between the variables listed above (e.g., do concentrations of certain elements increase with number percentages of ultrafine particles?)

4.0 Results and Discussion

In the following sections, results are first presented separately with respect to particle-level characteristics, metals and trace element concentrations, and 1-NP and PAH concentrations. Then, the correlational analysis between all dust variables is presented.

4.1 Sub- and Supramicron Particle Characteristics

Figure 4 shows the estimated sub- and supramicron particle densities for all 76 dust samples analyzed for this project. On average, submicron particles were found to be about 3x more abundant than supramicron particles – although the relative difference ranges from about 2-50x. It should be noted that any effects of particle size on deposition onto the sample filters has not been investigated, and is outside of the scope of this project. However, it is expected that any such effects may skew results shown here towards higher densities of relatively large particles, since they should experience greater force to deposit on the center of a filter in a two-piece, open face cassette (i.e., as was used for collection of these dust samples).

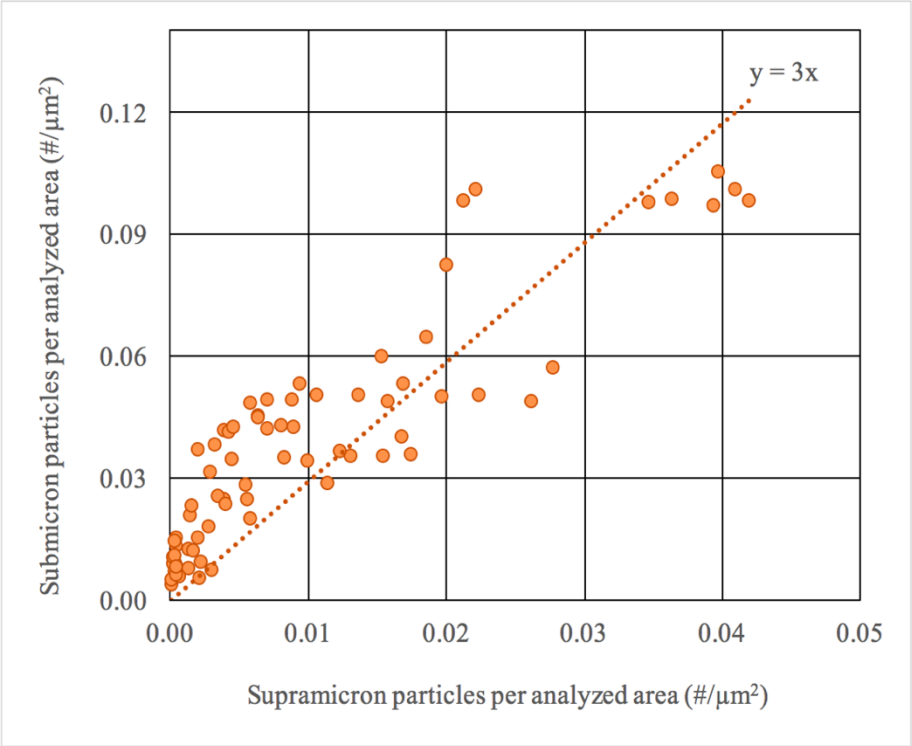

Figure 4. Estimated sub- versus supramicron particle density for all dust samples.

Figure 5 shows the sub- and supramicron particle densities by mine and sampling location. While these particle densities cannot necessarily be used to compute accurate values for average dust mass concentration, the two quantities should more or less trend together (i.e., higher particle densities should be associated with higher dust concentrations in the sampling environment). This figure clearly demonstrates that submicron particles dominated the dust samples collected across all mines and sampling locations. On average, the intake samples appear to have particularly high proportions of submicron particles.

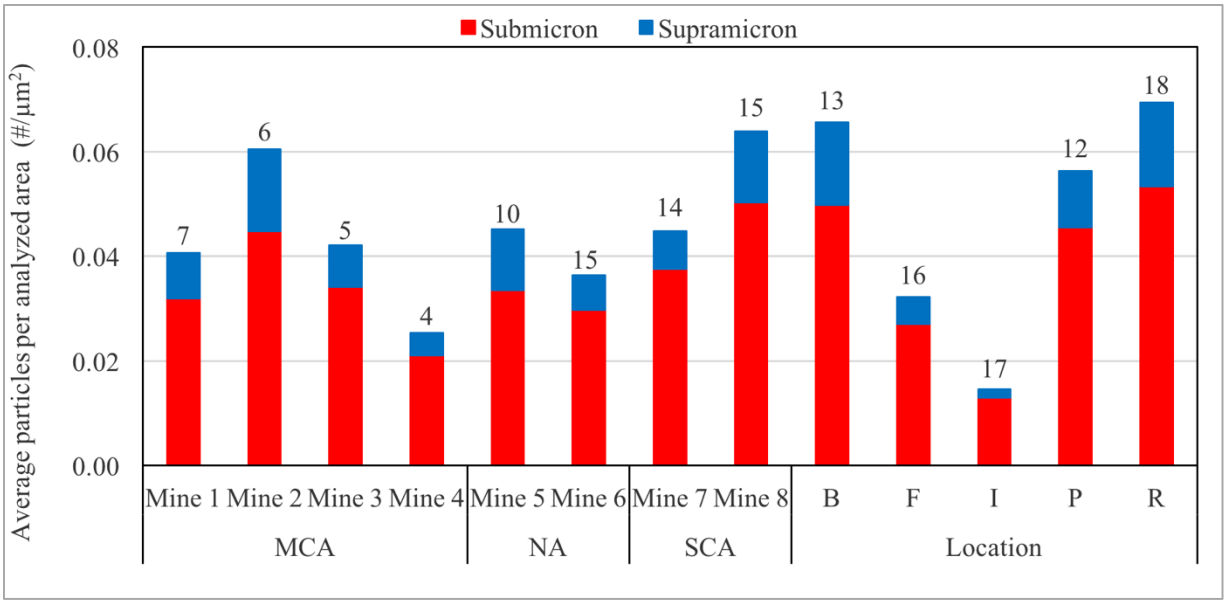

Figure 5. Average sub- and supramicron particle densities in each mine and sampling location. N values (i.e., number of samples analyzed from each mine or location) are shown above the bars.

During collection of the SEM-EDX data, it was observed that submicron particles classified into the C and HM mineralogy categories seemed to most often fall into the smallest size bin considered for this work – the ultrafine bin (i.e., 100-400 nm). On the other hand, submicron AS, Q and CB particles more often fell into the bins between 400-1,000 nm. These observations suggested that specific particle types (i.e., from specific sources) may have characteristically different size distributions. With this in mind, rather than continuing to split analysis at the generic sub/supra micron threshold, a decision was made to make the split between ultrafine particles and all larger particles. Upon merging the submicron particle data collected on this project with the supramicron data collected on the prior project, this decision led to analysis in three primary size ranges: ultrafines, larger particles (400-10,000 nm), and the entire size range (100-10,000 nm). These are the ranges discussed from here forward.

In order to explore the size distribution of particles in each mineralogy class, the weighted average particle size for each class was computed for every sample. This was done for the entire size range, and for the ultrafines and larger particles bins (Figure 6). In the figure, a very clear separation can be seen between the ultrafine and larger size bins for the C class. This observation supports the idea that ultrafine particles in this class may often be DPM rather than coal dust.

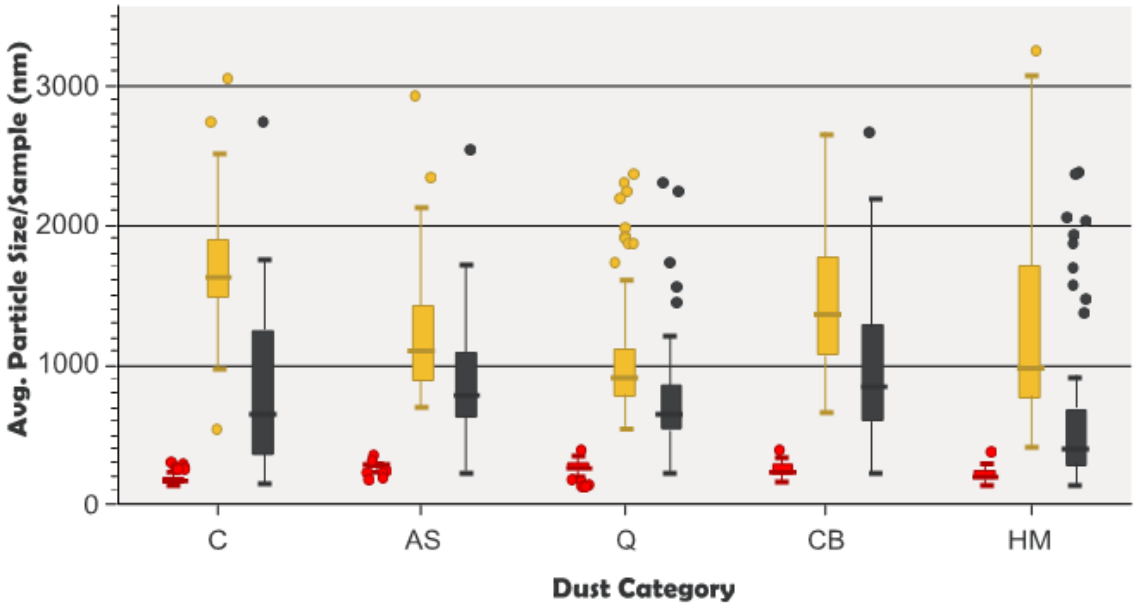

Figure 6. Average Box-and-whisker plot showing weighted average particle sizes per sample in each mineralogical (C: Carbonaceous, AS: Alumino-silicates, Q: Quartz, CB: Carbonate, HM: Heavy mineral.) Red data sets show particles in ultrafine size bin [100nm-400nm), yellow data sets show larger particle size bin [400nm-10000nm), and grey data sets show particles across the entire size range [100nm-10000nm).

Comparing the data for the total size range to the ultrafine or larger particles bins, Figure 6 also illustrates that the C and HM classes are more influenced, overall, by ultrafine particles than are the other mineralogy classes (i.e., for C and HM, the means of the grey data sets are relatively close to the means of the red data sets). This point is further highlighted in Table 6, which shows the mean of the weighted average particle size for each class and size bin, along with the percentage of particles in each bin. Ultrafine particles accounted for 72% of the total C particles and 82% of the total HM particles. There are several possible explanations for the presence of so many ultrafine HM particles, including the tendency for DPM to frequently have some associated metals content [Lee et al., 2006]. Moreover, there might be a tendency for HM particles generated from cutting geologic strata to be well liberated from host rock particles at relatively smaller sizes (e.g., HM grains are not obscured by occurrence with or within AS particles). Alternatively, there might be additional HM particle sources that have not been specifically identified heretofore (e.g., abrasion of drill or cutting bits).

Table 6. Means for weighted average particle size (nm) in ultrafine and larger particles size bins, and across the entire size range analyzed. For each category, the percentage of particles in the ultrafine and larger bins is also shown.

Size Category	Particle Size Bin	Dust Category				
		C	AS	Q	CB	HM
Ultrafine	[100nm-400nm)	189 (72%)	277 (37%)	260 (45%)	246 (41%)	208 (82%)
Larger	[400nm-10000nm)	1660 (28%)	1194 (63%)	1071 (55%)	1433 (59%)	1285 (18%)
Total	[100nm-10000nm)	834 (100%)	867 (100%)	742 (100%)	965 (100%)	623 (100%)

While the other mineralogy classes tend to have somewhat larger particles than the C and HM classes, Figure 6 and Table 6 show that significant numbers of ultrafine AS, Q and CB particles do occur in respirable coal mine dust. AS and Q particles should largely be associated with cutting or drilling rock strata in the mine. CB particles, based on our previous investigations of supramicron dust [e.g., Johann-Essex et al., 2017b], are thought to be associated more with application of rock dusting products (i.e., high-purity limestone or dolomite).

With respect to variability in particle mineralogy distributions between mines, Figure 7 shows the mean percentages of particles in each mineralogy class, broken down between the ultrafine and larger particles bins and for the entire size range. Based on the statistical testing procedures outlined in Section 3.4, Table 7 summarizes any statistically significant differences (at 95% confidence) found between mine means for specific mineralogy and/or size classes.

Ultrafine particles accounted for, on average, more than 50% of the total particle counts in all mines except for Mine 5; in Mine 6, more than 80% of the particles were ultrafine. Mine 6 was found to have statistically more ultrafine (and fewer larger) particles than Mines 5 and 8. No other statistically significant differences were found between the mean percentages of total ultrafine or total larger particles between mines (Table 7).

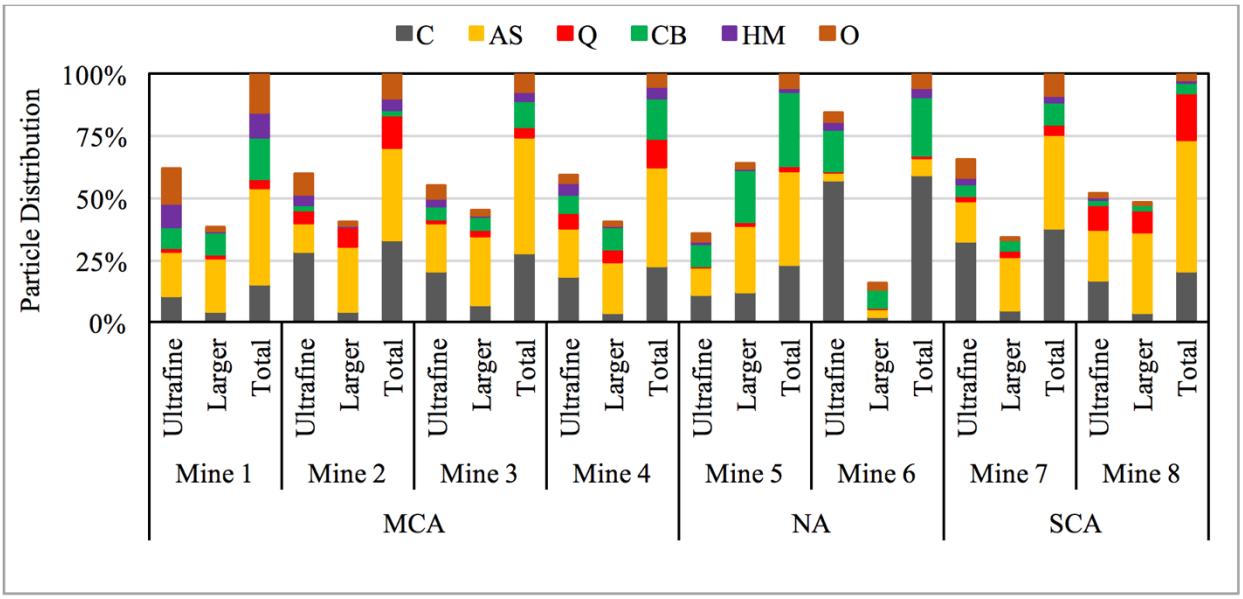

Figure 7. Average mineralogy distributions in the ultrafine (100-400 nm) and larger particles (400-10,000 nm) size bins, and across the total size range, for each mine. (C=carbonaceous, AS=alumino-silicate, Q=quartz, CB=carbonate, HM=heavy minerals, O=other.)

From Figure 7, the overall tendency to find more ultrafine C and HM particles (versus ultrafine AS, Q or CB particles) can also be clearly seen. In terms of statistically significant differences between mines, Mine 6 was found to have a higher mean percentage of ultrafine C particles than Mines 7 and 8. Mine 6 was known to be operating diesel equipment during sample collection, which may explain, at least in part, the relatively high numbers of ultrafine particles (particularly ultrafine C particles) found in this mine. The mean percentage of ultrafine HM particles in Mine 6 was moderate (i.e., third highest of any mine, after Mines 1 and 4). Mine 4 was the only other mine with known diesel equipment during sampling. It had the second highest mean percentages of

ultrafine C particles (after Mine 6) and ultrafine HM particles (after Mine 1); but the variability particle distributions between individual samples was very high in Mine 4 and consequently no statistically significant differences could be observed between dust characteristics in this and other mines.

Table 7. Summary of results from statistical analysis to identify significant differences (at 95% confidence) between particular mines or sampling locations based on their mean percentages of particles in various mineralogical classes and/or size bins. ND indicates that no statistically significant differences were found.

Class	Size Bin	Difference Found	
		Mines	Locations
All	Ultrafine	Mine 6 > Mines 5 and 8	ND
	Larger	Mine 6 < Mine 5 and 8	ND
C	Ultrafine	Mine 6 > Mines 7 and 8	I > B, P and R
	Larger	ND	ND
AS	Ultrafine	Mine 6 < Mines 1, 7 and 8	I < B and P
	Larger	Mine6 < Mines 5, 7 and 8	I < B and P
Q	Ultrafine	Mines 5 and 6 < Mine7 and 8	ND
	Larger	Mine 6 < Mines 7 and 8; Mine 5 < Mine 8	ND
CB	Ultrafine	Mine 2 < Mine 6; Mine 6 > Mines 7 and 8	ND
	Larger	Mine 2 < Mine 5	ND
HM	Ultrafine	ND	ND
	Larger	ND	ND
O	Ultrafine	Mine 1 > Mine 8	I > R
	Larger	ND	F > R

In contrast to the abundant C particles in Mine 6, it was found to have statistically lower percentages of AS particles than other mines (i.e., Mine 6 mean for ultrafine AS was lower than Mines 1, 7 and 8; and Mine 6 mean for larger AS particles was lower than Mines 5, 7 and 8). This observation is consistent with the relative ratio of coal and rock strata heights being cut in Mine 6 during dust sampling (i.e., the coal seam was relatively thick as compared to the total mining height as shown in Table 1). It is also noted that Mine 6 is a longwall operation, and strata cutting by a longwall shearer might produce dust with a different size distribution than cutting by a continuous miner. Mine 5 is the only other longwall operation represented in this study, and it had the second lowest mean value for ultrafine AS particles (after Mine 6) – though this was not found to be statistically different from the means in other mines. In general, there was substantial within-mine variability between AS percentages in both the ultrafine and larger particles size bins.

For Q particles, Mine 6 was found to have fewer ultrafine and larger particles than Mines 7 and 8; and Mine 5 was found to have fewer larger Q particles than Mine 8. The relatively low Q percentages in Mines 5 and 6, and higher percentages in other mines, is again consistent with the relative ratios of coal and rock strata being cut in the mines – and also the typical mass fractions of quartz observed in MSHA compliance sampling (Table 1). Notably, many of the highest single-sample percentages for ultrafine and larger Q particles were observed in Mines 2 and 4, but there was so much variability in dust from these mines that no statistical differences could be found between their mean Q values and those of other mines.

For the CB particle class, Mines 5 and 6 were observed to have the highest mean percentages of both ultrafine and larger CB particles. The mean percentage of ultrafine CB particles in Mine 6 was found to be statistically greater than that in Mines 2, 7 and 8; and the mean percentage of larger CB particles in Mine 5 was found to be greater than in Mine 2. This relative abundance of CB particles in Mines 5 and 6 is consistent with field observations of heavy rock dust application in these mines and our prior analysis of only the supramicron particles from the mines [Johann-Essex et al., 2017b]. Like for the C and AS classes, and the Q and HM classes in some mines, within-mine variability in the CB percentages was generally high.

Mineralogy class and size distributions were also compared with respect to sampling location (Figure 8, Table 6). The mean percentage of total ultrafine particles was highest for the I samples, although not statistically different from the other sampling locations. The I samples also had the highest mean percentage of ultrafine C particles, which was determined to be statistically greater than the means for the B, P, and R samples. This lends further support to the idea that many of the ultrafine C particles identified in this study were likely DPM. In intake airways, DPM should often make up a fairly large proportion of airborne particulates, along with perhaps particles sourced from rock dust application, due to the relative presence of DE (i.e., either from emissions in the mine such as from diesel-powered mantrips, or entrained in the intake air from emissions on the surface) and the relative absence of dust generation from cutting or drilling geologic strata. The I samples additionally had slightly higher, though not statistically different, means for ultrafine HM and ultrafine CB particles than samples from other locations; and the mean for larger CB particles was greater than that for all other locations except for R.

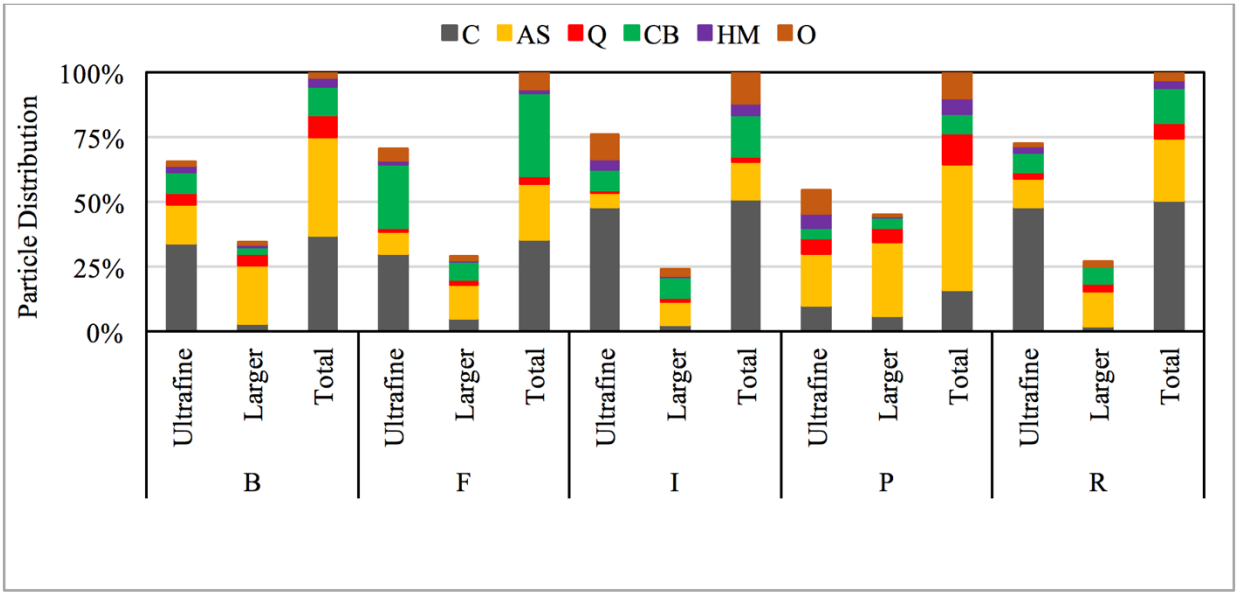

Figure 8. Average mineralogy distributions in the ultrafine (100-400 nm) and larger particles (400-10,000 nm) size bins, and across the total size range, for each sampling location. (C=carbonaceous, AS=alumino-silicate, Q=quartz, CB=carbonate, HM=heavy minerals, O=other.)

The P and F samples tended to have relatively more larger C particles than other locations (though no statistical difference observed between means), which is consistent with coal dust generating activities in the P and F locations (i.e., cutting at the face and breaking at the feeder, respectively).

Likewise, the samples from the B and P locations, where nearby activities are associated with cutting or drilling of rock strata, had the highest percentages of AS and Q particles in both the ultrafine and larger particle size bins. Mean percentages of ultrafine and larger AS particles in the B and P samples were found to be statistically greater than those for I samples.

The percentages AS and Q particles in both the ultrafine and larger particle size bins were also found to be relatively high in R samples, which are expected to be substantially influenced by production activities. Moreover, the R samples had high percentages of ultrafine and larger CB particles CB, which is consistent with heavy rock dust application in return airways to ensure sufficient inerting of coal dust fractions.

4.2 Metals and Trace Element Concentrations

The metals and trace elements analysis described in Section 3.2 was completed on a total of 74 respirable coal mine samples. For each sample, this analysis yielded values for potentially bioaccessible and total acid-soluble mass concentrations (mg/g) of 21 different elements. To review, the analytical method included two sequential digestions on each sample (i.e., first in SLF, then in strong acid). Potentially bioaccessible element concentrations were determined based on the mass the element that dissolved in the SLF; and total acid-soluble concentrations were determined from mass dissolved in the SLF plus the mass dissolved in the strong acid solution.

Based on the frequency of observation for each element (i.e., the relative number of samples for which it could be measured) and its relative range of concentrations, the elements were categories into four general groups: (1) major elements, which occurred frequently and at relatively high concentrations; (2) common trace elements, which occurred frequently but at relatively low concentrations; (3) rare trace elements, which occurred infrequently and at low concentrations; and (4) undetectable elements, which could not be measured in any samples. Figure 9 describes these four groups, and the tendencies for certain elements to be more or less bioaccessible. To visualize the observation frequency specifically for bioaccessible concentrations of any given element, Figures C1 and C2 (Appendix C) show an inventory of all samples by mine and location and identify those for which bioaccessible concentrations were measured.

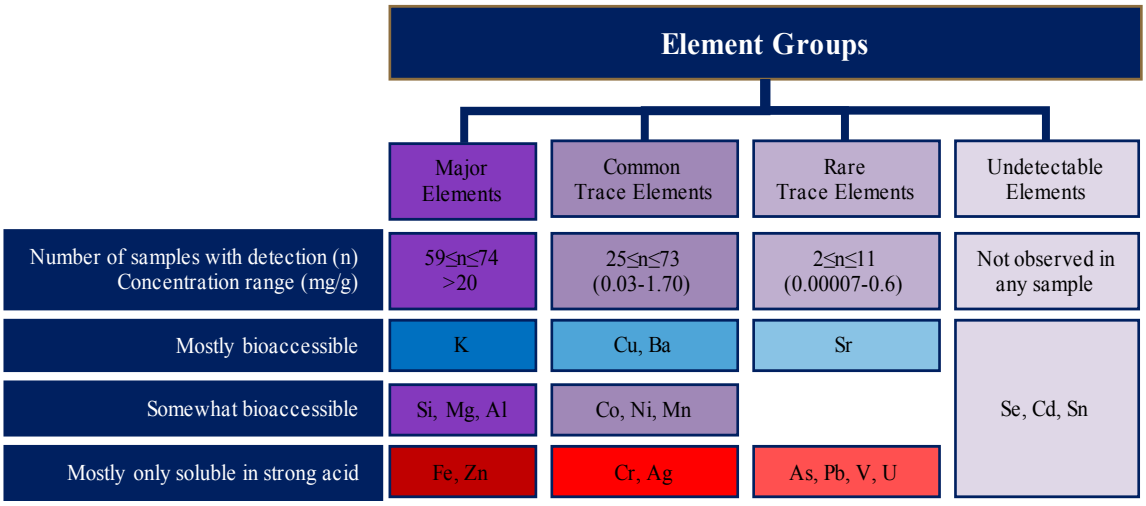

Figure 9. Description of four element groups based on the frequency of detection, general concentration range measured, and relative bioaccessibility of each element included in this study.

The major elements group includes K, Si, Mg, Al, Fe and Zn, each of which occurred in about 80% of the samples with total acid-soluble concentrations typically ranging between about 10-200 mg/g. K was the only element that was observed frequently, and at high potentially bioaccessible concentrations (i.e., nearly all of the total K concentration measured was dissolved in SLF). This is consistent with an understanding of typical K-bearing minerals, which tend to be relatively soluble. Si, Mg and Al were also observed in most samples and at relatively high concentrations, though they were only moderately bioaccessible (i.e., having 75%, 55%, and 26%, respectively, of their total concentrations dissolved in the SLF). Again, this is consistent with our understanding of typical rock strata (i.e., shales, slates and sandstones) from which dust (including significant AS particles) is commonly generated in the coal mines represented here. Significant Mg concentrations might additionally be contributed by rock dust application in the mines. It should be noted that Si concentrations measured here are expected to be largely related to AS particles, rather than Q particles, which should be highly insoluble. While Fe and Zn were also found at relatively high concentrations, they tended to be only slightly bioaccessible (i.e., 5% or less of the total concentration was dissolved in the SLF). These elements may too be associated with dust generated from geologic strata cutting or drilling in the mines, application of rock dust products; Fe has also been associated with DPM in some studies [see Lim et al., 2009]. It should be reiterated that the other primary elements expected to occur at high concentrations in coal mine dust (e.g., Ca, Na, S) could not be included in this analysis since they were also present at high concentrations in the digestion solutions.

The common trace elements group includes Cu, Ba, Co, Ni, Mn, Cr, and Ag (Figure 7), each of which were measured in at least one third of the samples, but at significantly lower total concentrations (i.e., generally in the range of about 0.1-5 mg/g, about 1-2 orders of magnitude less than the major elements). Within this group, Cu and Ba were observed to be mostly bioaccessible (i.e., having 90% and 100%, respectively, of their total concentrations dissolved in SLF). These elements may be associated with the geologic strata being cut or drilled in the mine and have also been measured in DE/DPM [e.g., see Zhou et al., 2014; Lim et al., 2009; USEPA, 2002; Spears at al., 1993; Zhao et al., 2015;]. Co, Ni and Mn were found to be moderately bioaccessible (i.e., 42%, 40%, and 30%, respectively, of their concentrations were dissolved in SLF). Mn, which frequently occurs with Fe, is presumably also associated with the mine geologic strata in most cases, but this metal can be present in DPM due to its presence in engine lubricants [Lim et al., 2009]. The source(s) of Co and Ni are unclear; they could be associated with geologic materials, DPM, rock dusting products, or abrasion of metal bits. Cr and Ag were also commonly occurring trace elements, though they were only slightly soluble in the SLF (i.e., less than 4% of their total concentration was dissolved in SLF). Again, the source(s) of these metals in coal mine dust is not clear. Either could be present in trace amounts in the mine geologic strata, and Cr is also commonly used as an alloying element to provide increased hardness and corrosion resistance to steel and has been associated with DE/DPM [USEPA, 2002].

Rare trace elements included Sr, As, Pb, V and U, each of which occurred in less than 15% of the samples – and generally at even lower concentrations than elements in the common trace elements group. When Sr was present, it was observed to be completely soluble in the SLF. The other elements in this group, however, were completely insoluble in SLF. Given that Sr is a relatively abundant element in the Earth's crust, and it is not known to be used in any products associated with use in coal mines, the Sr measured in a few samples here is most likely associated with the

geologic strata in the mine or the rock dusting products applied. As, Pb, V, and U may also be associated with geologic materials or rock dust products, and (except for U) are additionally known to occur in DPM [Lim et al., 2009]. Se, Cd, and Sn were all included in the metals and trace elements analysis, but none of these was measured in any of the samples at levels above the minimum reporting level (see Table B2).

For reference, Table 8 shows the average and maximum observed values for total acid soluble and potentially bioaccessible concentrations of each element measured in the mine dust samples. The table also shows permissible exposure limits (PELs) published by OSHA or other guidance for most of the elements.[4] The only element that clearly exceeded a PEL was Ag; its maximum total acid soluble concentration was just over the PEL. The maximum total acid soluble concentrations for Al, Fe, Mn and As were 64%, 82%, 41% and 71% of the PEL values. All other elements had maximum total acid soluble concentrations well below the PELs. Moreover, the average total acid soluble concentrations for all elements were 10% or less than the PELs.

Table 8. Projected airborne concentrations (µg/m3) of respirable elements in a coal mining environment based on the metals and trace elements analysis, and assuming a constant total respirable dust concentration of 1.5 mg/m3 and constant elemental concentrations in the dust. Values computed for maximum and average concentrations of total acid soluble and potentially bioaccessible elements. For reference, OSHA PEL values are also shown. PELs are established as TWAs on an 8-hour basis.

Element Groups	Element	OSHA PEL or other guidance		Mine Samples			
		µg/m^3	description	Avg total acid soluble	Avg potentially bioaccessible	Max total acid soluble	Max potentially bioaccessible
Major Elements	K	NL		42	42	388	388
	Si	NL		52	36	1180	750
	Mg	NL		65	36	1239	489
	Al	2000[1]	soluble	83	21	1282	532
	Fe	1000	soluble	106	5	816	66
	Zn	NL		54	1	750	15
Common Trace Elements	Cu	1000	dusts and mists	0.4	0.4	7.4	7.4
	Ba	500	soluble	0.5	0.5	9.8	9.8
	Co	20	metal, dust and fume	0.05	0.02	1.78	0.17
	Ni	100	metal and insoluble, or soluble	0.8	0.3	10.6	3.5
	Mn	200	compounds	2.5	0.7	81.1	14.9
	Cr	500	soluble	1.3	0.0	18.4	2.4
	Ag	10	metal and soluble	0.5	0.0	10.1	0.5
Rare Trace Elements	Sr	NL		0.9	0.9	62.9	62.9
	As	10	inorganic	0.15	0.00	7.06	0.00
	Pb	50	inorganic	0.13	0.00	8.65	0.02
	V	1000 14[2]	PEL for ferro-V is 1 mg/m^3 PEL for V_2O_5 is 0.05 mg/m^3	0.7	0.0	44.3	0.0
	U	200	soluble	0.000	0.000	0.004	0.000

[1] NIOSH recommended exposure limit for Al (soluble salts) is 2 mg/m^3 for an 8-hr TWA.
[2] PEL listed as 0.05 mg/m^3 as V_2O_5; this value has been converted to µg/m^3 as V for comparison to mine dust results.

[4] For elements where no PEL or recommendation has been established (e.g., Mg, Si and K), these are often captured by OSHA and MSHA under the umbrella terms of "nuisance dust" or "particulates not otherwise regulated," which generally have a respirable PEL of 5 mg/m^3 (on an 8-hr TWA basis).

It should be noted that, where PELs have been established, they are generally for particular forms of an element (e.g., as a metal, inorganic compound, soluble salt, etc.) While care has been taken to identify and tabulate PELs that may most closely apply to respirable coal mine dust samples, it is not possible (using the data collected for this project) to know how each element actually occurs in the dust particles. For example, depending on the source of V, it could occur as a natural mineral (i.e., within the mine geologic strata) or as ferro-V, which is a common alloying material for strengthening steel. No PEL appears to be available for V minerals but a value has been established for ferro-V; and much more conservative value is available for V_2O_5, which is used in ceramics manufacturing. As it is unlikely that V in these mine dust samples was present as V_2O_5, this PEL is included in Table 8 for comparative purposes.

As for the particle-level data, the metals and trace elements data was also studied to determine whether trends in dust characteristics could be observed on the basis of particular mines or sampling locations. Figure 10 shows the major elements group (Fe, Al, Mg, Si, Zn and K) results by mine. Mines 1, 2, 3, 4 and 5 generally tended to have the highest mean values for both potentially bioavailable and total acid soluble concentrations of most elements in this group. The exception was Zn, which was highest in samples from Mines 1, 5, 6 and 7. Despite the apparent trends in Figure 10, however, no statistically significant differences could be observed between the mines based on their mean values for potentially bioaccessible or total acid soluble concentrations for any of these elements (Table C1). This is attributed to high within-mine variability in concentrations for all of these elements. Interestingly, potential bioaccessibility of some elements also seems to vary between mines. For example, in most mines, nearly all of the total acid soluble Si in the dust was dissolved in the SLF, but only 30% of it was dissolved in SLF in Mine 4, and only 60% in Mine 5. This may be related to differences in the specific Si mineralogy between mines. Likewise, variability in the relative bioaccessibility of Fe, Al and to a lesser extent Mg are also apparent in Figure 10.

Figure 11 shows the major elements group results by sampling location. Again, some trends can be seen in the mean values – but no statistically significant differences were found (Table C1). Nevertheless, these results can support general hypotheses about the types of particles (and their possible sources) in different locations of a mine. For example, Fe and Al appear to trend together, with the highest mean concentrations in B and R locations, moderate mean concentrations in P and F locations, and the lowest mean concentration in the I location. The B and R locations also clearly have the highest mean concentrations of Mg and Si, though for these elements the I location have higher means that P and F locations. Moreover, the Si in the I location seems to be less bioaccessible than in other locations. Based on knowledge of particle generating activities in mines, these observations may indicate that geologic strata contribute most of the Fe and Al, but that Mg and Si may have additional major sources such as rock dusting products.

Figures 12 and 13 show the common trace elements group (Mn, Cu, Ba, Co, Ni, Cr and Ag) results by mine and sampling location, respectively; and analogous plots are presented for the rare trace elements group (Sr, V, As, Pb and U) in Appendix C (Figures C3 and C4). Based on the statistical analysis, the only significant differences found between mines were that Mine 3 had a higher total acid soluble V concentration than Mines 5, 6, 7 and 8; and that Mine 3 also had a higher total acid soluble As concentration than Mine 7 (Table C1). While not statistically significant, Figure 12 suggests that Mine 1 has relatively higher Mn and Ba than other mines, and Mines 1 and 2 have relatively higher Cr than other mines. The most notable trend in Figure 13 is that mean Mn concentrations trend similarly to Fe and Al, with the B and R locations having the highest concentrations, followed by the P and F locations, and then the I location.

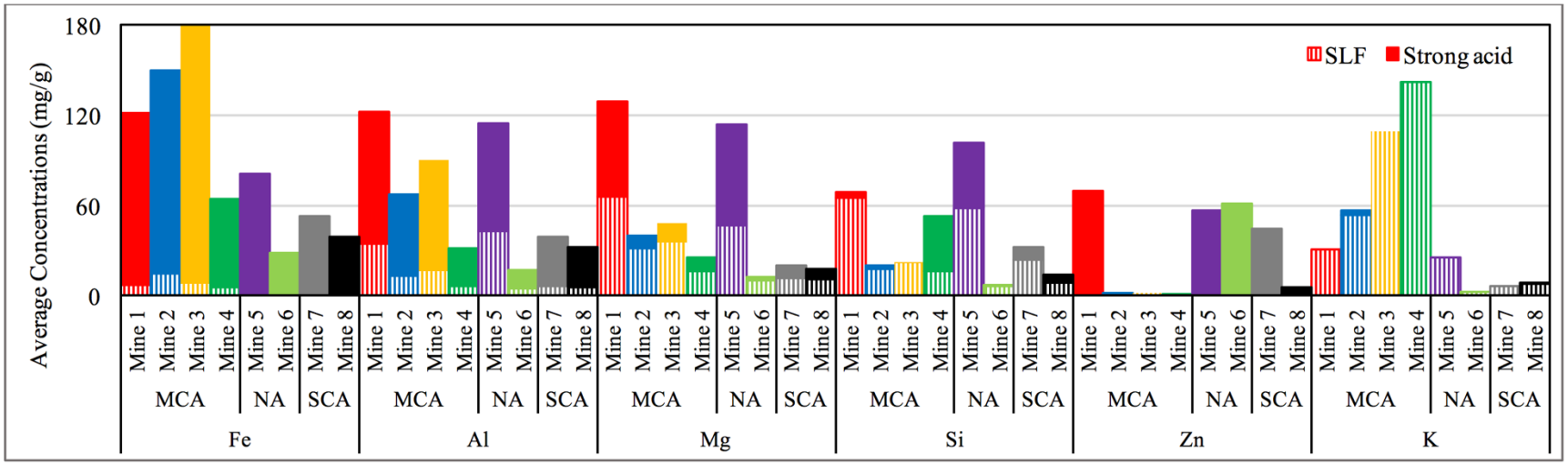

Figure 10. Average concentrations of major elements by mine. The total bar height shows the total acid soluble concentration, and the portion of the bar shown with a vertical pattern shows the potentially bioaccessible concentration (i.e., the portion dissolved in the SLF solution).

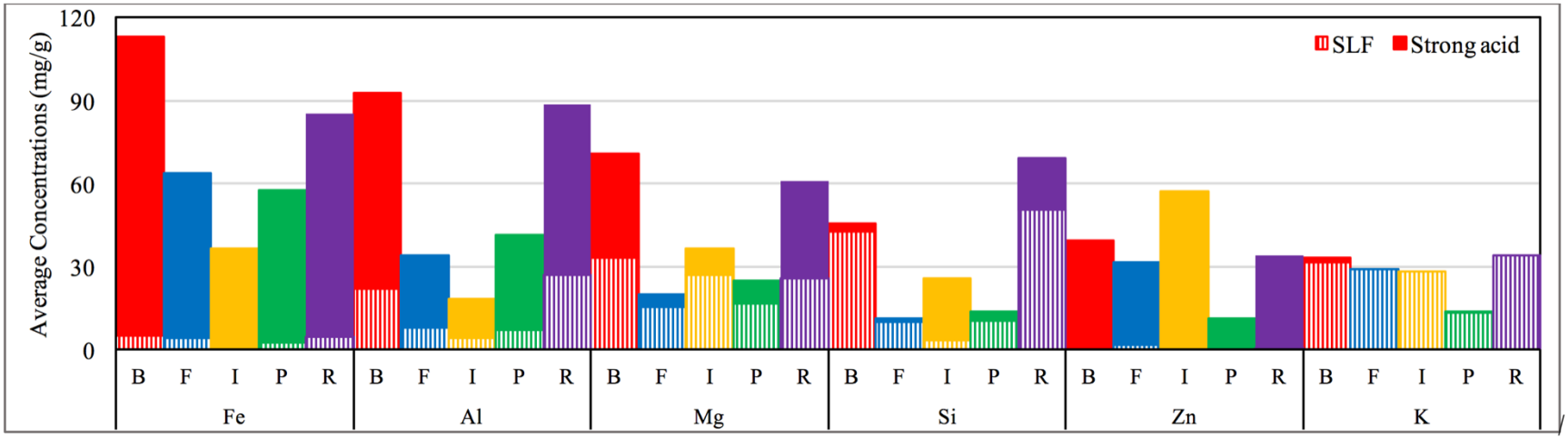

Figure 11. Average concentrations of major elements by sampling location (B=roof bolter, F=feeder, I=intake, P=production, R=return). The total bar height shows the total acid soluble concentration, and the portion of the bar shown with a vertical pattern shows the potentially bioaccessible concentration (i.e., the portion dissolved in the SLF solution).

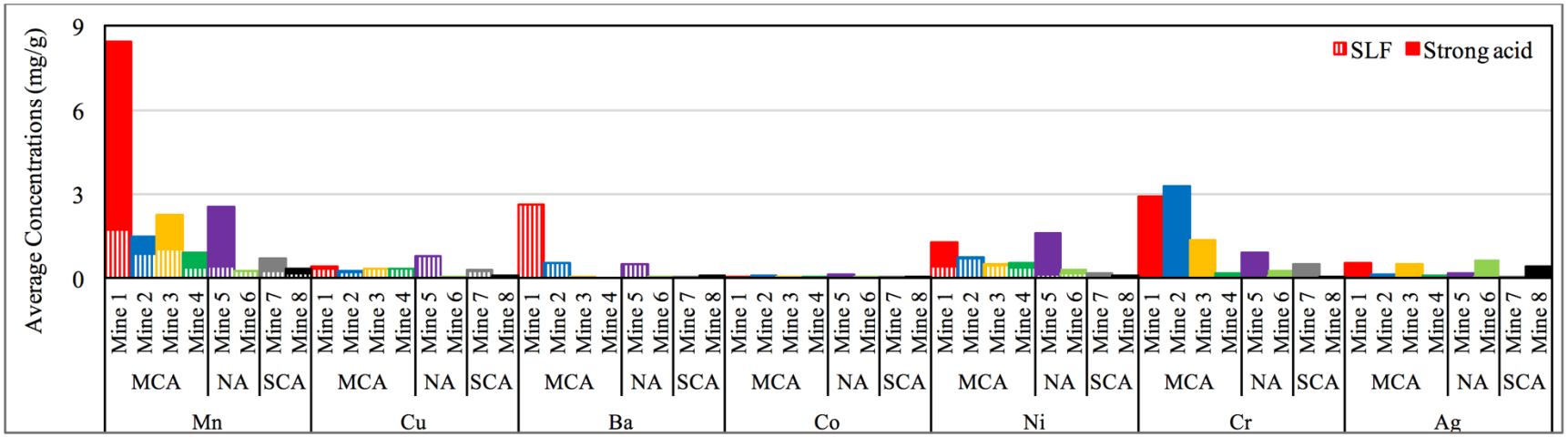

Figure 12. Average concentrations of common trace elements by mine. The total bar height shows the total acid soluble concentration, and the portion of the bar shown with a vertical pattern shows the potentially bioaccessible concentration (i.e., the portion dissolved in the SLF solution).

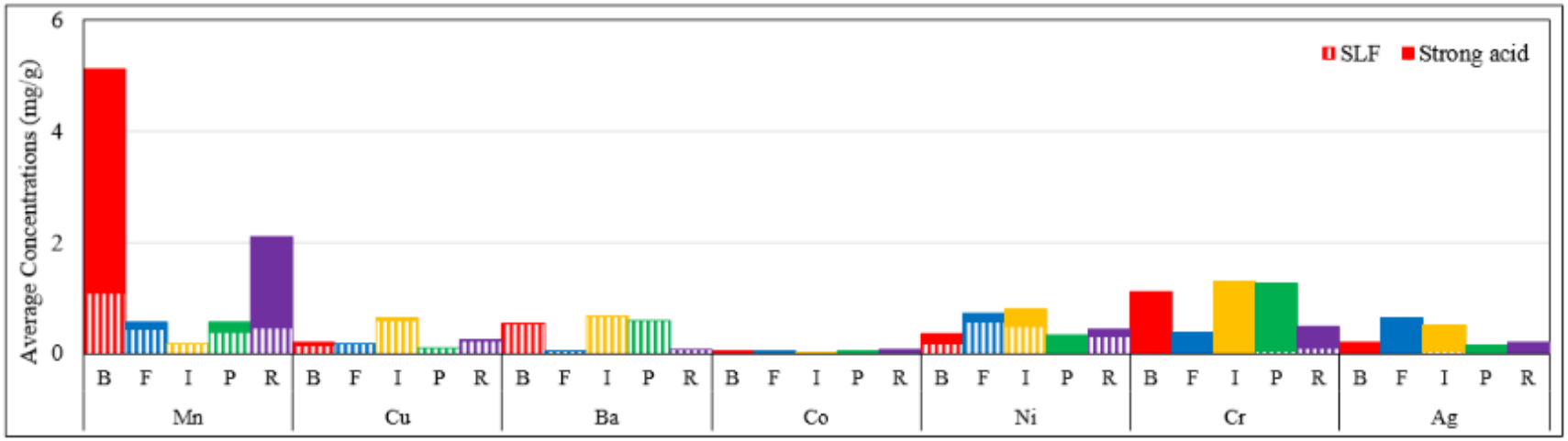

Figure 13. Average concentrations of common trace elements by sampling location (B=roof bolter, F=feeder, I=intake, P=production, R=return). The total bar height shows the total acid soluble concentration, and the portion of the bar shown with a vertical pattern shows the potentially bioaccessible concentration (i.e., the portion dissolved in the SLF solution)

4.3 1-NP and PAH Concentrations

Per Table 2, a total of 37 respirable mine dust samples were analyzed for PAHs and 36 were analyzed for 1-NP. Eight of the samples represented four pairs of replicates (all from Mine 4), and the results from each pair were averaged to obtain a single value for their respective sample sets. Additionally, lab-generated samples containing respirable particles from several raw and clean coal samples were also analyzed to gain insight into the possible contribution of coal dust to 1-NP and PAH concentrations in the mine samples. As mentioned in Section 3.3, results for PAHs presented here represent the total concentration of the 12 EPA PAHs that could be reliably quantified (see Table 5).

The lab-generated samples had very low or non-detectable levels of 1-NP. The highest concentration measured in any of these samples was 0.0007 µg/g, which was significantly lower than the concentrations measured in the mine samples. The average concentration of 1-NP in the mine samples was 0.071 µg/g, which is 100x more than in coal-dust only samples. The range of concentrations in the mine dust samples was 0.0003-0.2752 µg/g. These results provide further evidence that coal dust should not present analytical interferences for the measurement of 1-NP (i.e., as a DE/DPM surrogate).

Figure 14 shows the mean 1-NP concentration in each mine. In total 24 of 36 samples had measureable concentrations. Mines 4 and 6 were the only mines known to have operating diesel equipment at the time of dust sampling, and they both have relatively high 1-NP concentrations; however, the concentration in Mine 3 is even higher. 1-NP was also measured in Mines 2, 7 and 8. These results suggest that diesel equipment was probably operating in the mines during sampling. Anecdotally, we have observed that even when operators do not classify their mines as being "diesel mines", they generally still operate small pieces equipment (e.g., mantrips). Statistically significant differences between the mean 1-NP concentrations could not be found between any mines – nor between any sampling locations.

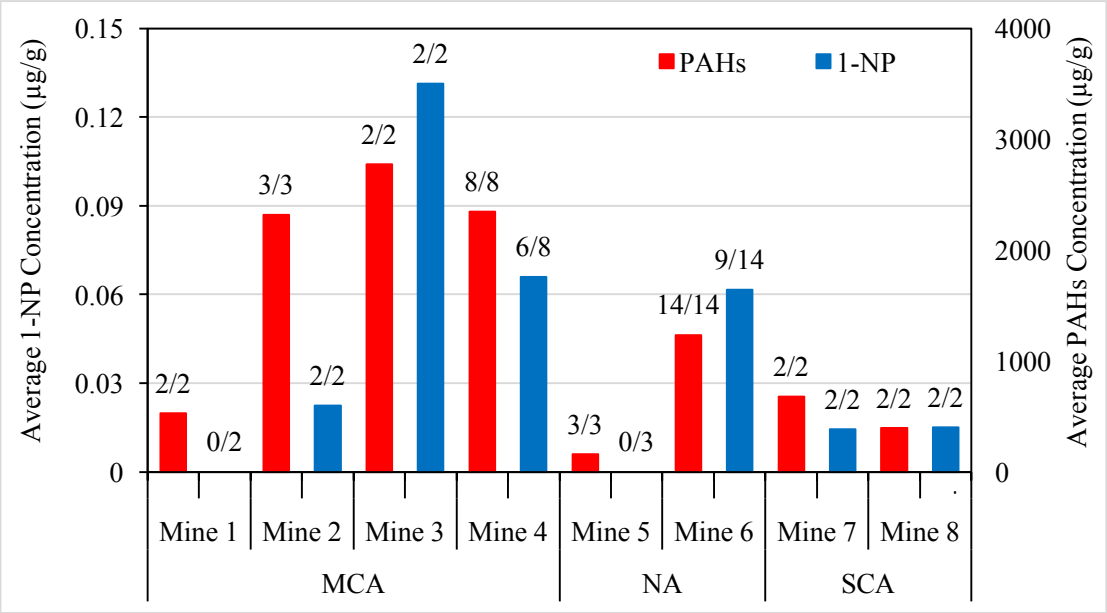

Figure 14. Average 1-NP and total PAHs concentrations by mine. Note separate axes. The numbers above each bar represent number of samples with measureable 1-NP or PAHs/total number of samples analyzed.

A comparison between the mean 1-NP concentrations by sampling location is shown in Figure 15. The highest mean concentration of 1-NP was in the I samples. Interestingly, these samples also had the lowest frequency of 1-NP observations (i.e., only 4 of 7 samples had measureable 1-NP), and notably none of the samples from Mines 1 and 5 (no measureable 1-NP in any samples) were from location I. Samples from location P had the lowest mean values of any location. To visualize the observation frequency for measurable concentrations of 1-NP, Figure D1 (Appendix D) shows an inventory of all samples by mine and location and identifies those for which 1-NP could be measured.

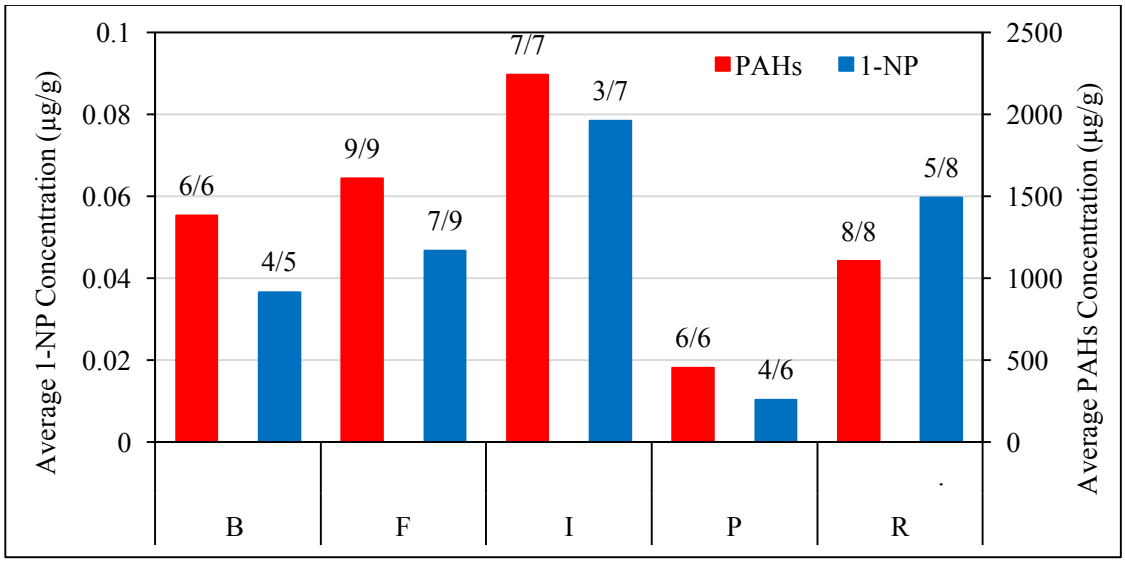

Figure 15. Average 1-NP and total PAHs concentrations by sampling location. Note separate axes. The numbers above each bar represent number of samples with measureable 1-NP or PAHs/total number of samples analyzed.

When analyzed for PAHs, the lab-generated samples had an average total PAH concentration of 71 µg/g, ranging from 50-109 µg/g. These samples were dominated by phenanthrene (average 48% of the total PAH mass), but had significant mass (4% or more) from seven other PAHs as well. The relationship between average mass percentages for all eight significant PAHs was: phenanthrene >> chrysene = benzo[g,h,i]perylene > pyrene > fluoranthene = benzo[a]anthracene = benzo[b]fluoranthene = benzo[a]pyrene. Together, these four compounds made up an average of 93% of the total PAH mass. The mine dust samples had an average total PAH concentration of 1,340 µg/g, ranging from 6-6,000 µg/g. Phenanthrene was again the dominant of the 12 PAHs quantified (average 71% of the total PAH mass), but just three other compounds represented 4% or more of the total PAH mass for the mine samples. The relationship between PAHs in this case was: phenanthrene >> pyrene > anthracene > fluoanthene. Together, these four compounds made up an average of 86% of the total PAH mass. While the relative ratios of individual PAHs was not further explored in this study, it may be a worthwhile topic of investigation for future studies.

The mean total PAHs concentrations by mine and sampling location are shown in Figures 14 and 15, respectively. Again, no significant differences could be found comparing mines or locations. In general, mean total PAH concentrations seems to correlate with mean 1-NP concentrations, with the exception of results from Mine 2 and the B sampling location, where the ratio of PAHs to 1-NP are relatively high. These observations appear to be related to several individual sample results with extraordinarily high total PAH concentrations, which skew the mean concentrations.

4.4 Correlational Analysis

A correlational analysis was performed to determine the presence and strength of correlations between the specific dust characteristics included in this study. Table 9 shows a correlation matrix for the following variables:

- Particle-level: Number percentage of total particles in the ultrafine (i.e., 100-400 nm) or larger particles size bin (i.e., 400-10,000 nm); and number percentage of ultrafine or larger particles in each defined mineralogy class (i.e., C, AS, Q, CB, and HM)
- Metals and trace elements: Mass concentration (mg/g) of potentially bioaccessibility or total acid-soluble elements (i.e., Al, Si, K, Fe, Zn, Cr, Mn, Co, Ni, Cu, Ag, Ba)
- 1-NP and PAHs: Mass concentration (µg/g) of 1-NP (n = 36) or the total PAHs

Based on Table 2, a total of 76 sample results were available for internal comparisons between particle-level variables; 74 samples results were available for internal comparisons between metals and trace elements variables, and with particle-level variables; and 31 sample results were available for internal comparisons between 1-NP and PAHs variables, and with the particle-level and metals and trace elements variables.

Table 9 confirms the strong correlations between total ultrafine particles the C and HM mineralogy classes. 1-NP and total PAHs are also positively correlated to these ultrafine particles, and are strongly correlated to one another (R=0.6). Additionally, some metals that may be associated with diesel exhaust (i.e., Zn, Cu, Ni, Cr) also show notable positive correlations to ultrafine C particles. Taken together, these findings provide further evidence to suggest that many ultrafine particles, including those with trace metals, are sourced from diesel emissions.

For larger particles, positive correlations were found for the AS and Q mineralogy classes and some of the major and common trace elements measured in this study (i.e., Fe, Al, Si, Mn, Co). These findings are generally consistent with expectations based on mine geologic strata given that much of the larger-sized dust appears to be mineral particles. Interestingly, while particles in the CB class had a relatively wide size distribution (i.e., not correlated with either ultrafines or larger size bins), they uniquely exhibited positive correlations to a suite of metals, namely Zn, Ag (for ultrafines) and Ag, Co, Ni, and Cr (for the larger particles). Considering that CB particles are thought to be largely sourced from rock dusting products, this observation suggests that the correlated metals are either associated with the rock dust material source itself (e.g., the geologic deposit from which it was mined), or the equipment used to produce (e.g., grinding mills, screens) or apply it (e.g., diesel-powered dusting machines).

In terms of comparisons within the metals and trace elements variables, the strongest positive correlations ($R \geq 0.5$) were observed between: bioaccessible Fe and Cr, Zn and Ag, Ba and Ni, Ba and Cr, and Ni and Cr. These relationships seem to suggest abrasion or corrosion of metal alloys as possible sources of particulates.

The negative correlations, or dichotomies between negative and positive correlations for a given variable, observed in Table 9 may also offer some valuable insights. For example, most of the mineralogy and size classes used to bin particles analyzed under the SEM tend to show clear positive correlations with some variables and clear negative correlations with others. In other words, some of the characteristics of particles in those classes can be clearly defined. For the total ultrafine, ultrafine C and HM, and total larger particles classes, this finding has already been explicitly discussed above. And the AS and Q classes follow a similar trend: they are positively

correlated with each other, Fe, Al, Si, and Mn, and negatively correlated with CB, HM, and Mg. The AS class is also negatively correlated with several trace metals like Zn, Co, Ni, Cr and Ag, as well as 1-NP. This stark contrast between the AS and Q classes and the (ultrafine) C and HM classes underscores not only the ability to comprehensively characterize respirable coal mine dusts, but also the distinct differences in particle types – and their likely sources. Unlike the other defined mineralogy classes, the CB and (larger) C and HM particle classes have few negative correlations with other variables – meaning particles in these classes are characterized much more by what they occur with, rather than what they occur without.

With respect to individual elements, aside from Fe, Al, and Si that tend to go with the AS and Q mineralogy classes, only Mg shows many negative correlations with other variables. Mg is negatively correlated with Si (particularly for potentially bioaccessible concentrations), Zn and K. This may indicate that samples with relatively high Mg concentrations were associated with very specific sources.

Table 9. Correlation matrix including particle size distributions (i.e., ultrafine="<400", larger particles="≥400nm") and dust category (C=Carbonaceous, AS=Alumino-silicates, Q=Quartz, CB=Carbonate, HM=Heavy minerals, O=Other);Mg, Al, Si, K, Cr, Fe, Mn, Co, Ni, Cu, Zn, Ag, and Ba element percentages as bioaccessible and total soluble concentrations; and total PAH and 1-NP concentrations. Color coding: gray indicate no notable correlation with R = [-0.2, 0.2], orange (weak) to red (strong) indicate negative correlation with R = (-0.2, -1.0], light green (weak) to dark green (strong) indicate positive correlation R = [1.0, 0.2). For strong correlations (R≤-0.5 or R≥0.5) cells have black outline.

R-Matrix		Tot.		C		AS		Q		CB		HM		Fe		Al		Mg		Si		Zn		K		Mn		Cu		Ba		Co		Ni		Cr		Ag		PAH	1-NP
		<400	>=400	<400	>=400	<400	>=400	<400	>=400	<400	>=400	<400	>=400	SLF	Tot.	SLF	Tot.	SLF	Tot.	SLF	Tot.	SLF	Tot.	SLF	Tot.	SLF	Tot.	SLF	Tot.	SLF	Tot.	SLF	Tot.	SLF	Tot.	SLF	Tot.	SLF	Tot.	Tot.	
Tot.	<400	1.0																																							
	>=400	-1.0	1.0																																						
C	<400	0.8	-0.8	1.0																																					
	>=400	-0.3	0.3	0.0	1.0																																				
AS	<400	-0.3	0.3	-0.6	0.0	1.0																																			
	>=400	-0.7	0.7	-0.7	0.0	0.7	1.0																																		
Q	<400	-0.1	0.1	-0.3	-0.2	0.3	0.2	1.0																																	
	>=400	-0.3	0.3	-0.3	-0.2	0.3	0.4	0.9	1.0																																
CB	<400	0.2	-0.2	0.1	-0.2	-0.5	-0.6	-0.3	-0.4	1.0																															
	>=400	-0.2	0.2	-0.1	-0.1	-0.5	-0.4	-0.3	-0.4	0.6	1.0																														
HM	<400	0.5	-0.5	0.3	-0.1	-0.3	-0.4	-0.2	-0.3	0.2	0.0	1.0																													
	>=400	0.2	-0.2	0.2	0.4	-0.1	-0.2	-0.2	-0.2	-0.1	-0.1	0.4	1.0																												
Fe	SLF	-0.3	0.3	-0.2	-0.1	0.1	0.2	0.2	0.4	-0.2	0.1	-0.2	-0.1	1.0																											
	Tot.	-0.5	0.5	-0.5	-0.1	0.4	0.5	0.2	0.3	-0.2	0.0	-0.3	-0.2	0.4	1.0																										
Al	SLF	-0.3	0.3	-0.4	0.2	0.1	0.2	0.0	0.0	0.1	0.1	-0.1	0.0	-0.1	0.0	1.0																									
	Tot.	-0.5	0.5	-0.5	0.0	0.5	0.6	0.4	0.4	-0.4	-0.3	-0.2	-0.1	0.0	0.2	0.5	1.0																								
Mg	SLF	0.4	-0.4	0.5	0.0	-0.4	-0.5	-0.3	-0.4	0.1	0.1	0.3	0.0	-0.3	-0.4	0.0	-0.2	1.0																							
	Tot.	0.2	-0.2	0.2	-0.1	-0.4	-0.3	-0.3	-0.3	0.2	0.2	0.3	0.1	-0.2	-0.4	0.2	0.1	0.7	1.0																						
Si	SLF	-0.3	0.3	-0.5	-0.1	0.5	0.5	0.3	0.3	-0.1	-0.2	-0.3	-0.1	0.1	0.3	0.1	0.4	-0.6	-0.4	1.0																					
	Tot.	0.1	-0.1	0.0	0.0	0.1	0.0	0.1	0.1	0.1	-0.2	-0.2	0.0	0.0	-0.2	-0.2	-0.1	-0.2	-0.1	0.5	1.0																				
Zn	SLF	0.3	-0.3	0.3	0.0	-0.3	-0.2	-0.1	-0.1	0.3	-0.1	0.0	0.1	-0.1	-0.2	-0.2	-0.3	0.0	0.1	0.0	0.5	1.0																			
	Tot.	0.3	-0.3	0.4	0.1	-0.2	-0.3	-0.1	-0.2	0.1	0.0	0.0	0.0	-0.1	-0.4	0.0	-0.4	0.2	-0.3	-0.1	-0.2	0.0	1.0																		
K	SLF	0.1	-0.1	0.1	0.0	0.0	-0.1	0.0	-0.1	-0.1	0.0	0.1	0.2	0.0	0.1	-0.5	-0.4	-0.4	-0.3	-0.4	-0.3	-0.1	0.0	1.0																	
	Tot.	0.1	-0.1	0.1	0.0	-0.2	-0.2	-0.1	-0.1	0.0	0.1	0.3	0.3	0.1	0.0	-0.4	-0.4	-0.3	-0.2	-0.3	-0.2	-0.1	-0.2	0.8	1.0																
Mn	SLF	-0.2	0.2	-0.3	0.1	0.3	0.3	0.1	0.2	-0.2	-0.2	0.1	0.1	0.3	0.3	0.2	0.3	-0.1	-0.1	0.1	-0.2	-0.1	0.1	-0.2	-0.2	1.0															
	Tot.	-0.4	0.4	-0.5	-0.2	0.4	0.5	0.3	0.3	-0.2	-0.1	-0.1	-0.2	0.4	0.4	0.2	0.4	-0.3	0.0	0.3	-0.1	-0.2	-0.3	-0.2	-0.2	0.6	1.0														
Cu	SLF	0.2	-0.2	0.3	0.0	-0.2	-0.2	-0.1	0.0	-0.1	0.0	0.1	0.1	-0.1	-0.3	-0.2	-0.3	0.3	0.1	-0.2	0.1	0.2	0.3	-0.1	0.0	-0.1	-0.2	1.0													
	Tot.	0.1	-0.1	0.2	0.1	-0.1	-0.1	-0.1	0.0	-0.1	0.0	0.1	0.4	-0.1	-0.2	-0.2	-0.3	0.1	0.1	-0.2	0.1	0.3	0.0	0.2	0.2	-0.1	-0.2	0.7	1.0												
Ba	SLF	0.1	-0.1	0.1	0.1	-0.2	-0.2	-0.1	0.0	0.0	0.0	0.2	0.1	-0.1	-0.2	-0.1	-0.2	0.2	0.2	-0.2	0.2	0.4	-0.1	-0.1	-0.1	-0.1	-0.1	0.1	0.2	1.0											
	Tot.	0.1	-0.1	0.1	0.1	-0.2	-0.2	-0.1	0.0	0.0	0.0	0.3	0.1	-0.1	-0.2	0.0	-0.1	0.2	0.2	-0.2	0.2	0.3	-0.1	-0.1	-0.1	-0.1	-0.1	0.1	0.1	1.0	1.0										
Co	SLF	0.1	-0.1	0.3	0.3	-0.2	-0.3	-0.1	-0.1	-0.1	0.0	-0.1	0.1	0.0	-0.2	0.0	-0.3	0.3	-0.1	-0.2	0.1	0.0	0.4	-0.2	-0.2	0.1	-0.2	0.0	-0.1	0.1	0.1	1.0									
	Tot.	-0.3	0.3	-0.2	-0.1	0.0	0.1	0.0	0.1	0.0	0.3	-0.2	-0.1	0.3	0.2	0.2	0.1	0.0	0.0	0.0	0.1	0.0	-0.2	-0.2	-0.1	-0.1	0.3	-0.1	-0.1	0.2	0.3	0.4	1.0								
Ni	SLF	0.2	-0.2	0.4	0.0	-0.4	-0.5	-0.2	-0.2	0.1	0.3	0.2	0.0	0.3	-0.3	-0.2	-0.4	0.2	0.1	-0.4	0.0	0.2	0.3	0.0	0.0	-0.1	-0.2	0.1	0.0	0.5	0.6	0.3	0.3	1.0							
	Tot.	0.0	0.0	0.0	0.0	-0.2	-0.2	-0.1	-0.1	0.2	0.3	0.0	0.0	0.0	-0.2	-0.1	-0.1	0.1	0.2	-0.2	-0.1	0.0	-0.1	0.2	0.2	-0.1	-0.1	0.0	-0.1	0.2	0.2	0.0	0.0	0.2	1.0						
Cr	SLF	-0.2	0.2	-0.1	-0.1	-0.1	-0.2	-0.1	-0.1	0.1	0.5	-0.1	-0.1	0.6	0.1	-0.1	-0.2	-0.1	0.0	-0.1	-0.1	0.0	-0.1	0.0	0.1	0.1	0.2	0.0	0.0	0.0	0.0	0.1	0.3	0.6	0.2	1.0					
	Tot.	0.2	-0.2	0.3	-0.1	-0.3	-0.4	-0.2	-0.1	0.1	0.2	0.2	0.0	0.2	-0.1	0.0	-0.1	0.3	0.4	-0.3	-0.1	0.1	-0.1	-0.2	-0.1	-0.2	-0.1	-0.1	-0.1	0.5	0.5	0.1	0.2	0.7	0.2	0.4	1.0				
Ag	SLF	0.0	0.0	0.0	-0.1	-0.3	-0.3	-0.1	-0.2	0.4	0.4	0.0	-0.2	-0.1	0.1	0.2	-0.2	0.2	0.2	-0.1	0.0	-0.1	-0.1	-0.1	-0.1	-0.2	0.0	0.0	0.0	0.1	0.1	-0.1	0.2	0.0	0.0	0.0	0.1	1.0			
	Tot.	0.2	-0.2	0.1	-0.1	-0.2	-0.2	-0.1	-0.1	0.5	0.0	0.1	-0.1	-0.1	-0.2	0.0	-0.1	0.1	0.1	0.0	0.3	0.7	0.0	-0.2	-0.1	-0.1	-0.2	0.0	0.0	0.0	0.0	-0.1	-0.2	0.0	0.0	0.0	0.0	0.0	1.0		
PAH	Tot.	0.3	-0.3	0.3	-0.2	0.0	-0.1	-0.2	0.0	0.0	-0.1	0.1	0.0	-0.1	-0.1	-0.2	-0.2	0.1	0.1	-0.3	-0.2	-0.1	-0.1	0.3	0.3	-0.2	-0.2	-0.2	-0.1	-0.2	-0.2	-0.1	-0.2	-0.1	-0.1	-0.1	0.0	-0.2	0.0	1.0	
1-NP		0.4	-0.4	0.4	-0.2	-0.3	-0.3	-0.1	-0.2	0.1	0.0	0.3	0.0	-0.2	-0.2	0.0	-0.1	0.1	0.2	-0.1	-0.3	-0.1	0.0	0.1	0.2	-0.3	-0.4	-0.1	-0.1	-0.2	-0.2	-0.1	-0.3	0.0	0.0	-0.1	0.3	-0.2	0.1	0.6	1.0
R-Matrix		Tot.		C		AS		Q		CB		HM		Fe		Al		Mg		Si		Zn		K		Mn		Cu		Ba		Co		Ni		Cr		Ag		PAH	1-NP
		<400	>=400	<400	>=400	<400	>=400	<400	>=400	<400	>=400	<400	>=400	SLF	Tot.	SLF	Tot.	SLF	Tot.	SLF	Tot.	SLF	Tot.	SLF	Tot.	SLF	Tot.	SLF	Tot.	SLF	Tot.	SLF	Tot.	SLF	Tot.	SLF	Tot.	SLF	Tot.	Tot.	

5.0 Publication Record and Dissemination Efforts

On conference presentation has been given on this project, and two journal publications are currently in preparation:

Keles, C., Johann, V. and Sarver, E. (2018) Comparison of Sub- and Supra-Micron Dust Particle Characteristics in Eight Appalachian Coal Mines, presented at the *2018 SME Annual Conference and Expo*, February 25-28, Minneapolis, MN, US.

Keles, C., Rezaee, M., and Sarver, E. Determination of potentially bioaccessible and total acid-soluble metals and trace elements in respirable coal mine dust materials, in preparation for *Aerosol and Air Quality Research*, (submission target date August 2018).

Sarver, E., Keles, C., and Rezaee, M. Submicron particles and trace constituents in respirable coal mine dusts, in preparation for the *International Journal of Coal Geology* (submission target date August 2018).

6.0 Conclusions and Impact Assessment

This project involved collection of a significant amount of data to describe respirable coal mine dust characteristics – many of which have heretofore not been widely investigated in field samples, let alone simultaneously. Together with the data collected on our prior Foundation-funded project (AFC113-11), the results presented here offer valuable insights to understand the whole composition and likely sources of particulates in coal mining environments. Key conclusions from this study include:

- There appear to be four major types of particles, each from a unique source, that can be present in coal mining environments like the ones represented here: (1) coal dust particles, generated from cutting of the coal strata and/or breakage and transport of mined coal materials; (2) mineral dust particles, which are generated from cutting or drilling of the rock strata surrounding the coal seam(s) and/or breakage and transport of mined rock materials; (3) dust particles associated with rock dusting products, which are generally dominated by carbonate minerals, and their application in the mine; and (4); particulates associated with emissions from diesel engines. The proportions of each of these particle types can vary significantly within and between mines, based on particle generating activities and source materials.
- Of the four defined particle types, diesel particulates appear to be mostly limited to the submicron range, whereas all other particle types can occur in both the sub- and supramicron ranges. While it is difficult to determine a typical size distribution for coal dust particles (i.e., due to interference from diesel particulates), it can be concluded that dust which is likely sourced from rock strata or rock dusting products can frequently occur in the smallest size range investigated here (i.e., "ultrafine", 100-400 nm). Overall, ultrafine particles (including diesel particulates) generally account for more than 50% of the total particle density; and submicron particles generally account for more than 75% of the total particle density.
- In general, dust particles associated with rock-strata sources (i.e., those classified as alumino-silicates or quartz) can be characterized by both positive and negative correlations with other dust variables (e.g., other mineralogy classes, specific elements); and the same is true for particles associated with diesel particulates (i.e., ultrafine carbonaceous or heavy mineral particles). This suggests that these particles often occur and dominate the respirable dust fraction under some particular conditions – an observation which may be useful in devising simple controls for limiting related exposures. On the other hand, coal dust particles and particles associated with rock dusting products exhibit primarily positive correlations to other dust variables, suggesting that they are more ubiquitous.
- Numerous metals and trace elements can be measured in respirable coal mine dusts, and some appear to occur in potentially bioaccessible forms (e.g., Al, Cu, Ba, Co, Ni, Mn). Based on the samples included in this study, however, measured metals and trace elements appear to occur at (total acid soluble) concentrations substantially below published (i.e., OSHA) permissible exposure limits. It is noted that such limits are not available for the bioaccessible concentration of studied elements, so no conclusions should be drawn here about the implications of these results.
- Metals and trace elements concentrations can vary greatly within a given mine, which may make comparisons between mines challenging. In some cases, correlations between

a specific element and other dust variables (e.g., dominant mineralogy class) may aid in identifying the source of the element.

- Consistent with expectations, 1-NP was well-correlated with other indicators of diesel exhaust in the mine dust samples studied here; and this provides further evidence in support of its possible use as a surrogate analyte for diesel exhaust and/or diesel particulates.
- In the mine samples studied here, total PAH concentrations (i.e., the sum of the 12 EPA PAHs measured) appeared to be generally related diesel exhaust, based on positive correlations with other variables indicative of diesel exhaust. It is possible that PAHs are also contributed to coal mine dust by the coal itself, though this was not fully explored in the current study.

The motivation behind this work was to serve coal miners, by searching for new insights to help promote healthy work environments. This project is directly related to the Foundation's *Disease Exposure and Risk Factors* focus area and the *Surveillance and Epidemiological Methods* research priority. The results and analysis presented here provide new and more complete information about the range of possible respiratory exposures in coal mines. Such information is key for furthering both epidemiological and medical studies, and for development of more robust health surveillance programs. Moreover, project findings should inform mining professionals and researchers interested in development of more effective environmental monitoring programs and/or respirable particulate prevention or mitigation strategies.

7.0 Recommendations for Future Work

While this and our prior dust characterization research have significantly expanded the understanding of respirable particulates in coal mine environments, there is much left to learn – and do. The following four areas appear particularly important for future work.

Health implications of particular coal mine dust constituents. Research is needed to investigate if or how exposure to certain dust constituents may impact health. This work might include study of individual particle types or elements, and also mixed or co-exposures (e.g., mineral dust and diesel particulates), which might lead to synergistic effects.

Relationships between specific particle/constituent characteristics and their sources. Especially for dust constituents with significant health implications, an effort should be made to identify the key sources. For example, which species are responsible for the bioaccessible fraction of a given elemental concentration; and what activities or materials in the mine environment are contributing them?

Improved monitoring capabilities to allow for measurement of particular dust constituents. The need for quartz-specific monitoring has long been recognized, and the ability to do this real-time is increasingly a priority. But as we learn more about other potentially important dust constituents, a more robust approach to monitoring seems prudent. Aside from capabilities to monitor for other specific constituents of concern (or their surrogates), capabilities that would allow for monitoring the whole composition of mine dust would represent a great advance.

Targeted controls to reduce exposures to particular dust constituents. The aim of deepening our understanding of respirable coal mine dust and our ability to monitor it in more meaningful ways is of course to identify risks, and then control them. Based on lessons learned until now, and those that may be learned through research into the above topics, improved dust control strategies should be devised and tested. For instance, our work has suggested that mining of rock strata can produce an inordinate amount of dust as compared to mining of coal strata. What sorts of controls might be engineered to further reduce dust generation during rock cutting, or other from other priority activities or sources?

8.0 References

Achten, C., & Hofmann, T. (2009). Native polycyclic aromatic hydrocarbons (PAH) in coals - a hardly recognized source of environmental contamination. *Science of the Total Environment, 407*(8), 2461-2473. http://dx.doi.org/10.1016/j.scitotenv.2008.12.008

Aneja, V. P., Isherwood, A., & Morgan, P. (2012). Characterization of particulate matter (PM 10) related to surface coal mining operations in Appalachia. *Atmospheric Environment, 54*, 496–501. http://dx.doi.org/10.1016/j.atmosenv.2012.02.063

Antao, V. C. dos S., Petsonk, E. L., Sokolow, L. Z., Wolfe, A. L., Pinheiro, G. A., Hale, J. M., & Attfield, M. D. (2005). Rapidly progressive coal workers' pneumoconiosis in the United States: geographic clustering and other factors. *Occupational and Environmental Medicine, 62*(10), 670-674. http://dx.doi.org/10.1136/oem.2004.019679

Agency for Toxic Substances and Disease Registry (ATSDR). (1995). Toxicological profile for Polycyclic Aromatic Hydrocarbons (PAHs). Atlanta, GA: U.S. Department of Health and Human Services, Public Health Service. Retrieved from: https://www.atsdr.cdc.gov/toxprofiles/tp69.pdf

ASTM D7439-14 Standard Test Method for Determination of Elements in Airborne Particulate Matter by Inductively Coupled Plasma–Mass Spectrometry, ASTM International, West Conshohocken, PA, 2014, https://dx.doi.org/10.1520/D7439-14

Attfield, M., & Seixas, N. (1995). Prevalence of pneumoconiosis and its relationship to dust exposure in a cohort of U.S. Bituminous coal miners and ex-miners. *American Journal of Industrial Medicine, 27*(1), 137-151.

Bezabeh, D. Z., Bamford, H. A., Schantz, M. M., & Wise, S. A. (2003). Determination of nitrated polycyclic aromatic hydrocarbons in diesel particulate-related standard reference materials by using gas chromatography/mass spectrometry with negative ion chemical ionization. *Analytical and Bioanalytical Chemistry, 375*(3), 381-388. http://dx.doi.org/10.1007/s00216-002-1698-8

Birch, M. E. & Noll, J. D. (2004). Submicrometer elemental carbon as a selective measure of diesel particulate matter in coal mines. *J Environ Monit, 6*(10), 799-806. http://dx.doi.org/10.1039/b407507b

Blackley, D. J., Crum, J. B., Halldin, C. N., Storey E., & Laney A. S. (2016). Resurgence of progressive massive fibrosis in coal Miners-Eastern Kentucky, 2016. *Morbidity and Mortality Weekly Report, 65*(49), 1385–1389.

Blackley, D. J., Halldin, C. N., & Laney, A. S. (2014). Resurgence of a debilitating and entirely preventable respiratory disease among coal miners. *Am J Respir Crit Care Med, 190*(6), 708-709. http://dx.doi.org/10.1164/rccm.201407-1286LE

Blackley, D. J., Reynolds, L. E., Short, C, Carson, R., Storey, E. S., Halldin, C. N., & Laney, A. S. (2018). Progressive Massive Fibrosis in Coal Miners from 3 Clinics in Virginia. *JAMA, 319*(5), 500-501. http://dx.doi.org/10.1001/jama.2017.18444

Brunner, T., Dahl, J., Obernberger, I., & Pölt, P. (2000). Chemical and structural analyses of aerosol and fly-ash particles from fixed-bed biomass combustion plants by electron microscopy. In Proceedings of the 1st world conference and exhibition biomass for energy and industry. Sevilla, Spain, ISBN 1-902916-15-8, Volume II, James&James Ltd. (ed), London, UK, pp.1991-1995.

Bugarski, A. D., Janisko, S. J., Cauda, E. G., Noll, J. D., & Mischler, S. E. (2011). Diesel aerosols and gases in underground mines: guide to exposure assessment and control. Pittsburgh, PA: U.S. Department of Health and Human Services, Public Health Service, Centers for Disease Control and Prevention, National Institute for Occupational Safety and Health, DHHS (NIOSH) Publication No. 2012-101 (RI 9687),1-159.
Retrieved from: https://www.cdc.gov/niosh/mining/UserFiles/works/pdfs/2012-101.pdf

Cabada, J. C., Rees, S., Takahama, S., Khlystov, A., Pandis, S. N., Davidson, C. I., & Robinson, A. L. (2004). Mass size distributions and size resolved chemical composition of fine particulate matter at the Pittsburgh supersite. *Atmospheric Environment, 38*(20), 3127-3141. http://dx.doi.org/10.1016/j.atmosenv.2004.03.004

Cohn, C., Laffers, R., Simon, S. R., O'Riordan, T., & Schoonen, M. A. (2006). Role of pyrite in formation of hydroxyl radicals in coal: possible implications for human health. *Particle and Fibre Toxicology, 3* (1), 16. http://dx.doi.org/10.1186/1743-8977-3-16

Dalal, N. S., Newman, J., Pack, D., Leonard, S., & Vallyathan, V. (1995). Hydroxyl radical generation by coal mine dust: Possible implication to coal workers' pneumoconiosis (CWP). *Free Radical Biology and Medicine, 18*(1), 11–20. http://dx.doi.org/10.1016/0891-5849(94)E0094-Y

Dean, J. R., Elom, N. I., Entwistle, J. A. (2017). Use of simulated epithelial lung fluid in assessing the human health risk of Pb in urban street dust. *Science of the Total Environment, 579*, 387-395. http://dx.doi.org/10.1016/j.scitotenv.2016.11.085

Donaldson, K., Li, X. Y., & MacNee, W. (1998). Ultrafine (nanometre) particle mediated lung injury. Journal of Aerosol Science, 29(5-6), 553–560. http://dx.doi.org/10.1016/S0021-8502(97)00464-3

Dubey, B., Pal, A. K., & Singh, G. (2012). Trace metal composition of airborne particulate matter in the coal mining and non–mining areas of Dhanbad Region, Jharkhand, India. *Atmospheric Pollution Research, 3*(2), 238-246. http://dx.doi.org/10.5094/APR.2012.026

Fedotov, P. S., Ermolin, M. S., Karandashev, V. K., & Ladonin, D. V. (2014). Characterization of size, morphology and elemental composition of nano-, submicron, and micron particles of street dust separated using field-flow fractionation in a rotating coiled column. *Talanta, 130*, 1-7. http://dx.doi.org/10.1016/j.talanta.2014.06.040

Furuta, N., Iijima, A., Kambe, A., Sakai, K., & Sato, K. (2005). Concentrations, enrichment and predominant sources of Sb and other trace elements in size classified airborne particulate matter collected in Tokyo from 1995 to 2004. *Journal of Environmental Monitoring*, *7*(12), 1155-1161. http://dx.doi.org/10.1039/b513988k

Gallagher, J., Heinrich, U., George, M., Hendee, L., Phillips, D. H., & Lewtas, J. (1994). Formation of DNA adducts in rat lung following chronic inhalation of diesel emissions, carbon black and titanium dioxide particles. *Carcinogenesis, 15*(7), 1291-1299.

Gamble, J. F., Reger, R. B., & Glenn, R. E. (2011). Rapidly Progressing Coal Workers Pneumoconiosis as a Confounding Risk Factor in Assessing Coal Mine Dust Safe Exposure Levels. *Journal of Clinical Toxicology*, S:1. http://dx.doi.org/ 10.4172/2161-0495.S1-003

Ghio, A. J., & Quigley, D. R. (1994). Complexation of iron by humic-like substances in lung tissue: role in coal workers' pneumoconiosis. *American Journal of Physiology, 267*(2 Pt 1), L173-L179. http://dx.doi.org/ 10.1152/ajplung.1994.267.2.L173

Gibson, P. (2016). Black lung's back? How we became complacent with coal miners' pneumoconiosis. *Australian Mining*, available at: https://australianmining.com.au/features/black-lungs-back-how-we-became-complacent-with-coal-miners-pneumoconiosis/

Guest, L. (1978). The endogenous iron content, by Mössbauer Spectroscopy, of human lungs—II. Lungs from various occupational groups. *Annals of Occupational Hygiene, 21*(2), 151-157. http://dx.doi.org/10.1093/annhyg/21.2.151

Harrington, A. D., Hylton, S., & Schoonen, M. A. A. (2012). Pyrite-driven reactive oxygen species formation in simulated lung fluid: Implications for coal workers' pneumoconiosis. *Environmental Geochemistry and Health, 34*(4), 527–538. http://dx.doi.org/10.1007/s10653-011-9438-7

Hartman, H. L., Mutmansky, J. M., Ramani, R. V., & Wang, Y. J. (2012). Mine ventilation and air conditioning. John Wiley & Sons, New York.

Huang, X., Gordon, T., Rom, W. N., & Finkelman, R. B. (2006). Interaction of iron and calcium minerals in coals and their roles in coal dust-induced health and environmental problems. *Reviews in Mineralogy & Geochemistry, 64*(1), 153–178. http://dx.doi.org/10.2138/rmg.2006.64.6

Huang, X., Luo, Y., & Luxbacher, K. (2013). Comments on "Coal workers' pneumoconiosis prevalence disparity between Australia and the United States". *Mining Engineering, 65*(2), 44-46.

Johann-Essex, V., Keles, C., Rezaee, M., Scaggs-Witte, M., & Sarver, E. (2017b). Respirable coal mine dust characteristics in samples collected in central and northern Appalachia. *International Journal of Coal Geology, 182*, 85-93. http://dx.doi.org/10.1016/j.coal.2017.09.010

Johann-Essex, V., Keles, C., & Sarver, E. (2017a). A Computer-Controlled SEM-EDX Routine for Characterizing Respirable Coal Mine Dust. *Minerals, 7*(1), 15. http://dx.doi.org/10.3390/min7010015

Julien, C., Esperanza, P., Bruno, M., & Alleman, L. Y. (2011). Development of an in vitro method to estimate lung bioaccessibility of metals from atmospheric particles. *Journal of Environmental Monitoring, 13*(3), 621–630. http://dx.doi.org/10.1039/c0em00439a

Kastury, F., Smith, E., & Juhasz, A. L. (2017). A critical review of approaches and limitations of inhalation bioavailability and bioaccessibility of metal(loid)s from ambient particular matter or dust. *Science of the Total Environment, 574*, 1054-1074. http://dx.doi.org/10.1016/j.scitotenv.2016.09.056

Kaufherr, N., & Lichtman, D. (1984). Comparison of micron and submicron fly ash particles using scanning electron microscopy and X-ray elemental analysis. *Environmental science & technology, 18*(7), 544-547. http://dx.doi.org/10.1021/es00125a012

Kim, K. H., Jahan, S. A., Kabir, E., & Brown, R. J. (2013). A review of airborne polycyclic aromatic hydrocarbons (PAHs) and their human health effects. *Environment International, 60*, 71-80. http://dx.doi.org/10.1016/j.envint.2013.07.019

Kittelson, D. B. (1998). Engines and Nanaoparticles: A Review. *Journal of Aerosol Science, 29*(5), 575-588. http://dx.doi.org/10.1016/S0021-8502(97)10037-4

Langrish, J. P., Frampton, M. W., & Blomberg, A. (2011). Human exposure studies. In Cardiovascular effects of inhaled ultrafine and nano-sized particles. Edited by: Cassee, F. R.; Mills, N. L.; Newby, D. E., John Wiley & Sons, Hoboken, NJ.217-239.

Lee, D. G., Miller, A. L., Park, K. H., & Zachariah, M. R. (2006). Effects of Trace Metals on Particulate Matter Formation in a Diesel Engine: Metal Contents from Ferrocene and Lube Oil, *Int J Automot Techn, 7*(6), 667-673.

Li, T., Wang, Y., Li, W. J., Chen, J. M., Wang, T., & Wang, W. X. (2015). Concentrations and solubility of trace elements in fine particles at a mountain site, southern China: regional sources and cloud processing. *Atmospheric Chemistry & Physics, 15*, 8987-9002. http://dx.doi.org/10.5194/acp-15-8987-2015

Lim, J., Lim, C., & Yu, L. E. (2009). Composition and size distribution of metals in diesel exhaust particulates. *Journal of Environmental Monitoring, 11*, 1614-1621. http://dx.doi.org/10.1039/b822514a

Liu, J., Liu, G., Zhang, J., Yin, H., & Wang, R. (2012). Occurrence and risk assessment of polycyclic aromatic hydrocarbons in soil from the Tiefa coal mine district, Liaoning, China. *Journal of Environmental Monitoring, 14*(10), 2634-2642. http://dx.doi.org/10.1039/c2em30433c

Maiti, S. K., & Mishra, A. K. (2013). Airborne inhalable heavy metals concentration in coal mining and non-mining areas in India: A review. *Indian Journal of Environmental Protection*, 33(6), 491-499.

McKenna, J. D., Turner, J. H., & McKenna Jr, J. P. (2008). Fine particle (2.5 microns) emissions: regulations, measurement, and control. John Wiley & Sons. New York.

Miller-Schulze, J. P., Paulsen, M., Toriba, A., Hayakawa, K., & Simpson, C. D. (2007). Analysis of 1-nitropyrene in air particulate matter standard reference materials by using two-dimensional

high performance liquid chromatography with online reduction and tandem mass spectrometry detection. *Journal of Chromatography A, 1167*(2), 154–160. http://dx.doi.org/10.1016/j.chroma.2007.08.026

Minitab 18 [Computer software]. (2018), Retrieved from: http://support.minitab.com/en-us/minitab/18/

Mischler, S. E., Cauda, E. G., Di Giuseppe, M., McWilliams, L. J., St. Croix, C., Sun, M., Franks, J, & Ortiz, L.A. (2016). Differential activation of RAW 264.7 macrophages by size-segregated crystalline silica. *Journal of Occupational Medicine and Toxicology. 11*, 57. http://dx.doi.org/10.1186/s12995-016-0145-2

Mitsche, S., Poelt, P., & Wagner, J. (2006). Analysis of submicron particles by scanning electron microscopy-energy-dispersive X-ray spectrometry-accuracy of size measurement. *Scanning, 28*(5), 282–288. https://dx.doi.org/10.1002/sca.4950280507

MSHA, Federal Register, 66, 5526-5706 (2001).

MSHA, Federal Register, 71, 28924-29012 (2006).

Niu, J., Rasmussen, P. E., Hassan, N. M., & Vincent, R. (2010). Concentration distribution and bioaccessibility of trace elements in nano and fine urban airborne particulate matter: Influence of particle size. *Water, Air, and Soil Pollution, 213*(1-4), 211-225. http://dx.doi.org/10.1007/s11270-010-0379-z

Oberdörster, G., Oberdörster, E., & Oberdörster, J. (2005). Nanotoxicology: An Emerging Discipline Evolving from Studies of Ultrafine Particles. *Environmental Health Perspectives*, *113*, 823-839. http://dx.doi.org/10.1289/ehp.7339

Pan, Y., Tian, S., Li, X., Sun, Y., Li, Y., Wentworth, G. R., & Wang, Y. (2015). Trace elements in particulate matter from metropolitan regions of Northern China: Sources, concentrations and size distributions. *Science of the Total Environment, 537*, 9–22. http://doi.org/10.1016/j.scitotenv.2015.07.060

Pandey, P., Patel, D. K., Khana, A. H., Barman, S. C., Murthy, R. C. & Kisku G. C. (2013). Temporal distribution of fine particulates (PM2.5, PM10), potentially toxic metals, PAHs and Metal-bound carcinogenic risk in the population of Lucknow City, India. *Journal of Environmental Science and Health, Part A: Toxic/Hazardous Substances and Environmental Engineering*. *48*(7), 730-745. http://dx.doi.org/10.1080/10934529.2013.744613

Pelfrêne, A., Cave, M., Wragg, J., & Douay, F. (2017). In Vitro Investigations of Human Bioaccessibility from Reference Materials Using Simulated Lung Fluids. *International Journal of Environmental Research and Public Health, 14*(2),112. http://dx.doi.org/10.3390/ijerph14020112

Poelt, P., Schmied, M., Obernberger, I., Brunner, T., & Dahl, J. (2002). Automated analysis of submicron particles by computer-controlled scanning electron microscopy. *Scanning, 24*(2), 92-100. http://dx.doi.org/10.1002/sca.4950240207

Riley, E. A., Carpenter, E. E., Ramsay, J., Zamzow E., Pyke, C, Paulsen M. H., Sheppard, L., Spear, T. M., Seixas, N. S., Stephenson, D. J., & Simpson, C. D. (2018). Evaluation of 1-Nitropyrene as a Surrogate Measure for Diesel Exhaust. *Ann Work Expo Health, 62*(3), 339-350. http://dx.doi.org/10.1093/annweh/wxx111

Samara, C., & Voutsa, D. (2005). Size distribution of airborne particulate matter and associated heavy metals in the roadside environment. *Chemosphere, 59*(8), 1197–1206. http://dx.doi.org/10.1016/j.chemosphere.2004.11.061

Sapko, M. J., Cashdollar, K. L., & Green, G. M. (2007). Coal dust particle size survey of US mines. *Journal of Loss Prevention in the Process Industries*, *20*(4-6), 616-620. http://dx.doi.org/10.1016/j.jlp.2007.04.014

Schauer, J. J. (2003). Evaluation of elemental carbon as a marker for diesel particulate matter. *Journal of Exposure Analysis and Environmental Epidemiology, 13*(6), 443–53. http://doi.org/10.1038/sj.jea.7500298

Scheepers, P. T. J., & Bos, R. P. (1992). Combustion of diesel fuel from a toxicological perspective. *International Archives of Occupational and Environmental Health, 64*(3), 149-161. https://dx.doi.org/10.1007/BF00380904

Scheepers, P. T. J., Martens, M. H. J., Velders, D. D., Fijneman, P., Kerkhoven, M. van, Noordhoek, J., & Bos, R. P. (1995). 1-nitropyrene as a marker for the mutagenicity of diesel exhaust-derived particulate matter in workplace atmospheres. *Environmental and Molecular Mutagenesis, 25*(2), 134–147. https://dx.doi.org/10.1002/em.2850250207

Scheepers, P. T. J., Micka, V., Muzyka, V., Anzion, R., Dahmann, D., Poole, J., & Bos, R. P. (2003). Exposure to dust and particle-associated 1-nitropyrene of drivers of diesel-powered equipment in underground mining. *The Annals of Occupational Hygiene, 47*(5), 379-388. https://dx.doi.org/10.1093/annhyg/meg036

Sellaro, R., Sarver, E., & Baxter. D. (2015). A Standard Characterization Methodology for Respirable Coal Mine Dust using SEM-EDX. *Resources, 4*(4), 939–57. http://dx.doi.org/ 10.3390/resources4040939

Shang, D., Kim, M., & Haberl, M. (2014). Rapid and sensitive method for the determination of polycyclic aromatic hydrocarbons in soils using pseudo multiple reaction monitoring gas chromatography/tandem mass spectrometry. *Journal of Chromatography A, 1334*, 118-125. http://dx.doi.org/ 10.1016/j.chroma.2014.01.074

Sharkey Jr, A. G., Kessler, T., & Friedel, R. A. (1975). Trace elements in coal dust by spark-source mass spectrometry. S.P. Babu (Ed.), *Trace Elements in Fuel* (pp. 48-56). Washington D.C.: American Chemical Society. http://dx.doi.org/10.1021/ba-1975-0141.ch004

Spears, D. A., & Martinez-Tarazona, M. R. (1993). Geochemical and mineralogical characteristics of a power station feed-coal, Eggborough, England. *International Journal of Coal Geology, 22*, 1-20. http://dx.doi.org/10.1016/0166-5162(93)90035-9

Suarthana, E., Laney, A. S., Storey, E., & Attfield, M. D. (2011). Coal workers' pneumoconiosis in the United States: regional differences 40 years after implementation of the 1969 Federal Coal Mine Health and Safety Act. *Occup Environ Med., 68*(12), 908–913. http://dx.doi.org/10.1136/oem.2010.063594

Talaska, G., Underwood, P., Maier, A., Lewtas, J., Rothman, N., & Jaeger, M. (1996). Polycyclic aromatic hydrocarbons (PAHs), nitro-PAHs and related environmental compounds: biological markers of exposure and effects. *Environmental health perspectives*, 104(5), 901-906.

Environmental Protection Agency [USEPA]. (2002). Health assessment document for diesel engine exhaust. Prepared by the National Center for Environmental Assessment, Washington, DC, for the Office of Transportation and Air Quality; EPA/600/8-90/057F.

U.S. Environmental Protection Agency [USEPA]. (2007). EPA Method 3546 Microwave Extraction. EPA/3546/R-0/1.

World Health Organization (WHO). (2012). IARC: Diesel engine exhaust carcinogenic. IARC Monographs on the evaluation of carcinogenic risks to humans. Lyon, France
Retrieved from: https://www.iarc.fr/en/media-centre/pr/2012/pdfs/pr213_E.pdf

Zamengo, L., Barbiero, N., Gregio, M., & Orrù, G. (2009). Combined scanning electron microscopy and image analysis to investigate airborne submicron particles: A comparison between personal samplers. *Chemosphere, 76*(3), 313–323.
http://dx.doi.org/10.1016/j.chemosphere.2009.03.065

Zhao, L., Ward, C. R., French, D., Graham, I. T. (2015). Major and trace element geochemistry of coals and intra-seam claystones from the Songzao Coalfield, SW China. *Minerals, 5*, 870-893. http://dx.doi.org/10.3390/min5040531

Zhou, C., Liu, G., Cheng, S., Fang, T., Lam, P. K. S. (2014). The Environmental geochemistry of trace elements and naturally radionuclides in a coal gangue brick-making plant. *Scientific Reports*, *4*(6221), 9. http://dx.doi.org/10.1038/srep06221

Zosky, G. R., Hoy, R. F., Silverstone, E. J., Brims, F. J., Miles, S., Johnson, A. R., Gibson, P. G., & Yates, D. H. (2016). Coal workers' pneumoconiosis: an Australian perspective. *Med J Aust.*, *204*(11), 414-418. http://dx.doi.org/10.5694/mja16.00357

9.0 Appendices

Appendix A – Manual SEM-EDX Routine for Submicron Particle Analysis

For the submicron analysis, the environmental SEM is operated under high vacuum conditions at a voltage of 10kV, with a spot size of 4.0µm, magnification of 20,000x, and at the optimal working distance of 12.5 mm. The instrument is operated in backscatter mode.

- After the SEM instrument is set to the above operating conditions, the routine begins at the center frame and then proceeds through the other frames respectively (from frame 1 to 45, see Figure A-1) to ensure analysis across a wide area. At 20,000x magnification, each frame is approximately 139 μm^2 (12.67 µm x 10.96 µm) and the frames are spaced 1 mm apart.

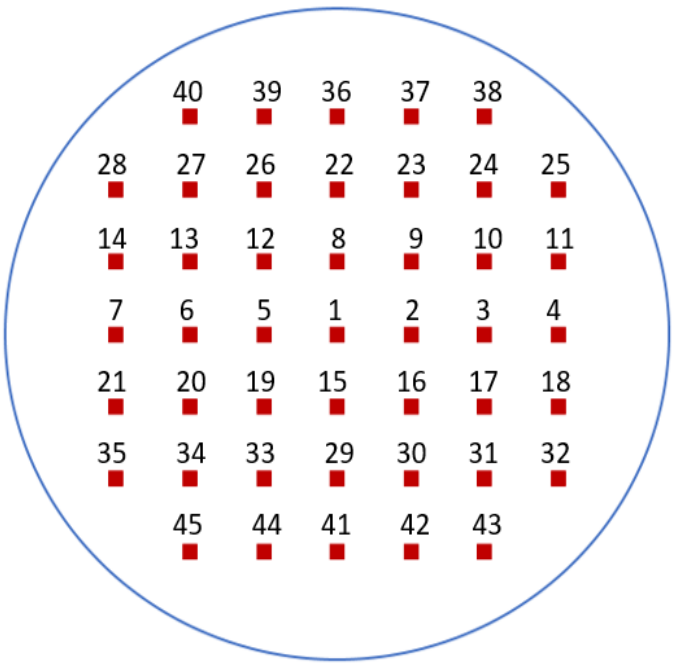

Figure 16. Frame positions on the subsample filter. The blue circle represents a 9-mm diameter subsample taken from the center of a 37-mm filter sample.

- In each frame, seven particles are analyzed (i.e., the first four are in the upper left quadrant of the frame; and the last three are in the lower right quadrant, see Figure A-2). This means that the maximum number of particles selected for analysis is 315 (i.e., 7 particles per frame in 45 frames). For each particle, the long and intermediate dimensions are measured, and then EDX elemental spectral peak heights (cps/eV) are recorded for the following elements: C, Al, Si, Ca, Mg, Fe, Ti, S, K, Na, P, Cr, Ni, Cl, Mn, Cu, Zn, Pb, Hf, Co, and F. Using these peak heights, the particle can be binned into one of the pre-defined mineralogical classes (i.e., C, AS, Q, CB, HM) or into the O class.

- If submicron particle loading on the sample is relatively light, the upper right and lower left quadrants in each frame are used to identify additional particles (i.e., up to a total of 7 per frame). Further, more frames may be analyzed beyond the 45 shown in Figure A-1 if necessary;

in this case, frames are located equidistant between the those identified in Figure A-1 and following the same pattern (i.e., analysis begins between frames 1 and 2).

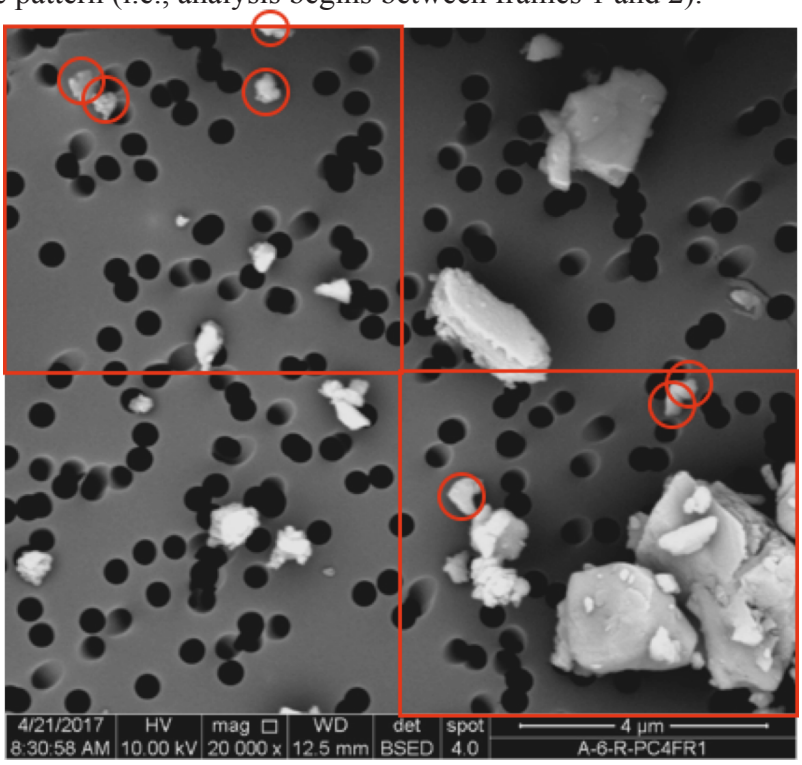

Figure 17. Quarter frames (red rectangles) and particles used in analysis (particles in red circles) for this particular frame.

Appendix B – Method for determination of potentially bioaccessible metals and trace elements in respirable dust samples

Removal of dust from filters:

- Loaded filters are weighed to establish a pre-dust removal weight.
- Support pads are removed from the cassettes and weighed filters are placed back into the cassettes. The cassettes are closed tightly.
- Inlet plug of the cassettes is opened and 2-3 ml of 18MΩ water is pipetted into the cassette. The plug is closed, and the cassette is shaken to loosen the dust from the filter. Next, the inlet plug is removed, and then the upper piece of the cassette is opened to avoid water splashing from the cassette. The filter is carefully removed and placed into a digestion tube, and the remaining water and dust inside the cassette are pipette into the digestion tube while rinsing the filter. An additional 2 mL of water is pipette into the cassette for further rinsing, and then transferred by pipette into the digestion tube again while rinsing the filter. More water is pipetted if is necessary to rinse and completely cover the filter inside the tube.
- The prepared tubes are capped and sonicated for 1 hour and then centrifuged for 10 mins (3000 rpm) to settle the dust to the bottom of the tube.
- Caps of the tubes are opened and filters are pulled close to top of the tube (i.e., not touching the water surface) using clean tweezers. The uncapped tubes are placed into the oven @110°C. When the filters are dry, they are removed from the tubes and placed into petri dishes, and they are weighed when cool down. The tubes remain in the oven until all water evaporates.
- Recovered dust is calculated by subtracting the clean filter weight from the loaded weight.

Preparation of simulated lung fluid (SLF):

- Lung fluid is simulated by preparing "Gamble's solution" or similar, per Pelfrene et al., 2017.
- The water bath is filled with 18MΩ water and heater of the water bath is set to 37°C.
- To prepare 1 Lt of SLF, 1 Lt of DI water is poured into a beaker, and 5 ml of the water syringe out to rinse the weighing boat at the end of the preparation.
- The magnetic stirrer bar is put inside the beaker and the beaker is located on the magnetic stirrer.
- The magnetic stirrer is turned on and the stirring level is increased slowly to avoid splashing.
- The weighing boat is tared and required amount of chemical is weighed and poured into the beaker and after it is dissolved into the water, weighing boat is tared again for the second chemical and so on. Each chemical is added in required amount. Order of the chemicals is also important. The chemical list, order of chemicals and concentration of each chemical are listed in Table B1.
- All chemical compounds in SLF solution are in solid form except trace metal grade sulfuric acid. Density of sulfuric acid is 1.84 g/cm³ ($1g/cm^3=10^6 mg/L$) so required sulfuric acid volume is 27.7µL.
- After all the chemicals are poured into the beaker, syringe the 5 ml of 18MΩ water back by rinsing the weighing boat to wash any remaining chemicals into the beaker.

- The beaker with SLF is located inside of the 37°C water bath. Solution of SLF must have pH of 7.4, but it is around 8-9. In order to decrease it to 7.4, trace metal grade HCl is added into the solution. Ph-meter is calibrated prior to each usage.

Table 10. SLF solution chemistry

Addition	Chemical	Formula	Concentration/L
1	Ammonium chloride	NH_4Cl	535mg
2	Sodium chloride	NaCl	6780mg
3	Sodium bicarbonate	$NaHCO_3$	1770mg
4	Sodium carbonate	Na_2CO_3	630mg
5	Sodium dihydrogen phosphate monohydrate	$NaH_2PO_4 \cdot H_2O$	166mg
6	Sodium citrate dihydrate	Na_3-citrate$\cdot 2H_2O$	59mg
7	Glycine	$C_2H_5NO_2$	450mg
8	Sulfuric acid	H_2SO_4	51mg/L=27.7µL
9	Calcium chloride dihydrate	$CaCl_2 \cdot 2H_2O$	29mg

Modified analytical method to estimate potentially bioaccessible concentrations of metals and other trace elements in respirable dust:

- Julien et al. (2011) claimed that in order to estimate bioaccessibility of metals solid to liquid ratio can be taken between 1/500 and 1/50,000. The dust samples generally have low weights (i.e., below 1mg) and to get at least 5ml solution, the liquid needs to be as much as possible. For this reason, in this study, solid to liquid ratio is taken as 1/50,000. Based on this ratio, required amount of SLF is added in to the digestion tubes.
- The tubes are located into the sonication bath for 24 hours at 37°C.
- After sonication, the tubes are centrifuged for 10mins at 3000rpm to settle down the dust to the bottom of the tubes.
- The 5 ml of the liquid (SLF + Respirable dust) inside the tubes is syringed into the ICP tubes using PTFE filter. By this way, if there are any dust particles, they are hold by the filter and only particles that can dissolved inside the SLF or particles less than 0.1um can pass through the filter.
- 100 µl of trace metal grade nitric acid is added to the ICP tubes for preservation and they are ready for the ICP analysis.

Modified analytical method to estimate total acid-soluble concentrations of metals and trace elements in respirable dust:

- This method is based on ASTM D7439-14
- The PTFE filters used to collect dust from SLF solution is placed into the digestion tube that used in previous steps. The filter, filter holder and walls of the digestion tube are washed by pipetting ($1HNO_3+9H_2O$) diluted nitric acid under hood. Water is used in this process is 18MΩw water.
- The hot block is located under hood. The tubes are placed into hot block at 120°C (the internal temperature inside the tube is 95°C.) and the top of the tubes are covered with plastic watch glass.
- The digestion tubes are heated until inside of the tubes is completely dry.

- 1.25 mL of concentrated hydrochloric acid is added to each digestion vessel, and vessels are covered with a plastic watch glass. The digestion vessels are placed in the hot block apparatus and heat at an internal temperature of 95°C for 15 minutes. Then, they are removed from the hot block for 5 mins to cool down.
- 1.25 mL of concentrated trace metal grade nitric acid is added to each digestion vessel, and the plastic watch glasses are replaced. The digestion vessels are placed in the hot block apparatus and heat at an internal temperature of 95°C for 15 minutes. Then, they are removed from the hot block for 5 mins to cool down. The hot block is turned off.
- The watch glass is removed from each digestion vessel and washed down into the digestion vessel with 18MΩ water.
- Each sample is diluted to a final volume of 25 mL with 18MΩ water. The water is added slowly to avoid spattering. The vessels are capped and liquid inside the vessels is mixed by shaking the tubes.
- The digestion tubes placed into the turned-off hot block for 5mins while it has still some heat.
- 5 ml of the solution inside the digestion vessels are syringed into the ICP tube using PTFE syringe filters, and acidified to 2% HNO_3.
- For each ICP run, at least 5 blank PC filters are prepared using both SLF and acid digestion procedures mentioned above to avoid background effects and allow correct elemental component estimations in the samples.

ICP-MS analysis:

- The analysis was conducted using a Thermo Electron X-Series ICP-MS.
- ICP results (µg/L in the digestate solution analyzed) are blank corrected and then transformed into a dry dust concentration (µg/g) using the dust mass recovered from a filter. The concentration determined from the SLF digestate is regarded as potentially bioaccessible; and the sum of the concentration from the SLF and strong acid digestates is regarded as total acid-soluble concentration.
- The elements that were measured by ICP-MS are listed in Table B2 with their respective method reporting level (MRL) in the ICP solution. These limits are based on the calibration curve for each element, which is generated using a series of standard solutions. The limits of detection are generally about one order of magnitude lower. It should be noted that some elements included in the ICP measurements were not considered here. These are: Cl, P, Na, Ca, S, Ti and Mo. Since the SLF solution itself includes significant Cl, P, Na, Ca and S, these elements may not be reliably estimated using the ICP-MS analysis. Significant amounts of P can also affect Ti estimation. Moreover, the ICP-MS instrument used here was found to not be accurately calibrated for Mo.

Table 11. MRL for each element in ICP-MS sample. Elements in red were not considered here.

MRL (µg/L)	Element	MRL (µg/L)	Element
0.05	U	10	Fe, Mg, Si, Sr, V, Zn
0.1	Co, Ni, Ag	50	Ba, Ca, Mo, P
0.5	As	100	K, Na
1	Al, Cd, Cr, Cu, Pb, Mn, Ti	200	Cl
5	Se	1000	S

Preparation of lab-generated dust samples:

For preliminary work to test the metals and trace elements analytical method, lab-generated dust samples were used. These were made using the following procedure.

- All lab-generated samples are collected using standard equipment for respirable dust sampling in coal mines. Escort ELF pumps are calibrated to a flow rate of 1.7 L/min, and used with 10mm Dorr-Oliver cyclones (i.e., to discard particles greater than 10µg, and achieve roughly 50% capture of particles approximately 4µm). Samples are collected using two-piece plastic cassettes on 37mm PC filters. PC filters are placed into the cassette on the top of a support pad to prevent filter from tearing or moving inside the cassette.
- Before dust collection, all blank PC filters used in dust collection are weighed and initial weights are recorded.
- After each dust type is collected, the cyclone parts and tubing are washed and wiped thoroughly, and dried by blowing air inside the parts and tubing.
- Filter and support pad loaded cassettes are assembled with cyclones, tubing and pumps and attached inside a dust box. The entire assembly operated under a working fume hood. The required powder material (i.e., raw coal, clean coal, or rock dust, etc.) is poured into the bottom of the box and the top of the box is covered with another plastic bag to minimize the dust release outside the box. All pumps are turned on and compressed air is blown into the box to aerosolize the dust. During this process, the respirable size dust is collected on the filter.
- After dust is collected, cassettes are completely closed (i.e., inlet and outlet) and the outside of the cassettes are cleaned with air and damp paper towels to avoid contamination during sample preparation for ICP analysis.

Appendix C – Additional Results for Metals and Trace Elements Analysis

Table 12. Summary of results from statistical analysis to identify significant differences (at 95% confidence) between particular mines or sampling locations based on their mean percentages of potentially bioaccessible or total acid soluble element concentrations. ND indicates that no statistically significant differences were found.

Element	Concentration	Differences Found	
		Mines	Locations
Mg	Potentially bioaccessible	ND	ND
	Total acid soluble	ND	ND
Al	Potentially bioaccessible	ND	ND
	Total acid soluble	ND	ND
Si	Potentially bioaccessible	ND	ND
	Total acid soluble	ND	ND
K	Potentially bioaccessible	ND	ND
	Total acid soluble	ND	ND
V	Potentially bioaccessible	ND	ND
	Total acid soluble	Mine 3 > Mines 5, 6, 7 and 8	ND
Cr	Potentially bioaccessible	ND	ND
	Total acid soluble	ND	ND
Fe	Potentially bioaccessible	ND	ND
	Total acid soluble	ND	ND
Mn	Potentially bioaccessible	ND	ND
	Total acid soluble	ND	ND
Co	Potentially bioaccessible	ND	ND
	Total acid soluble	ND	ND
Ni	Potentially bioaccessible	ND	ND
	Total acid soluble	ND	ND
Cu	Potentially bioaccessible	ND	ND
	Total acid soluble	ND	ND
Zn	Potentially bioaccessible	ND	ND
	Total acid soluble	ND	ND
As	Potentially bioaccessible	-	-
	Total acid soluble	Mine 3 > Mine 7	ND
Ag	Potentially bioaccessible	ND	ND
	Total acid soluble	ND	ND
Ba	Potentially bioaccessible	ND	ND
	Total acid soluble	ND	ND

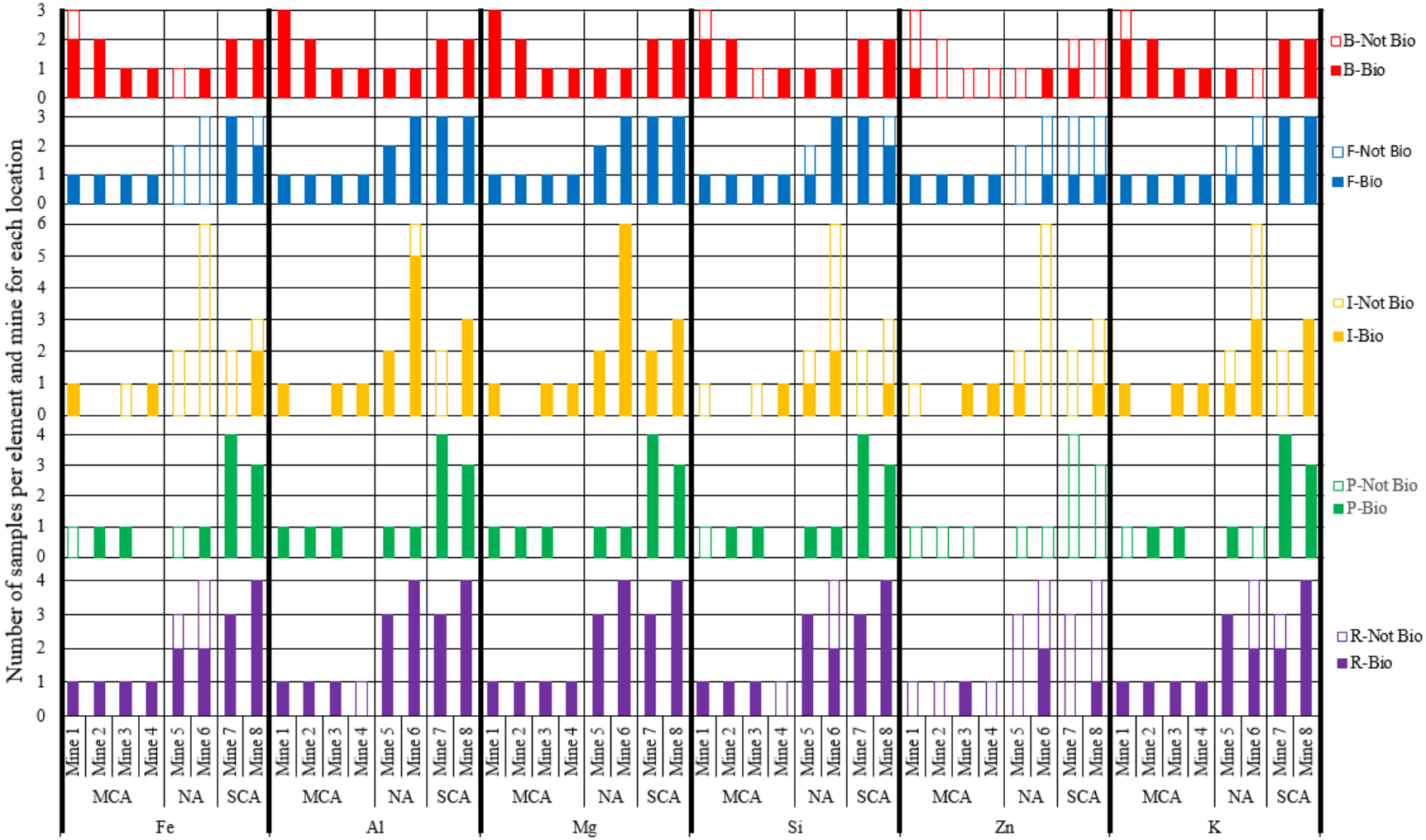

Figure 18. Total number of samples by mine and sampling location (B=roof bolter, F=feeder, I=intake, P=production, R=return), with number of samples having potentially bioaccessible concentrations of major elements also identified (i.e., by filled bars). For example, a total of three B samples were analyzed from Mine 1, two of which had potentially bioaccessible Fe concentrations.

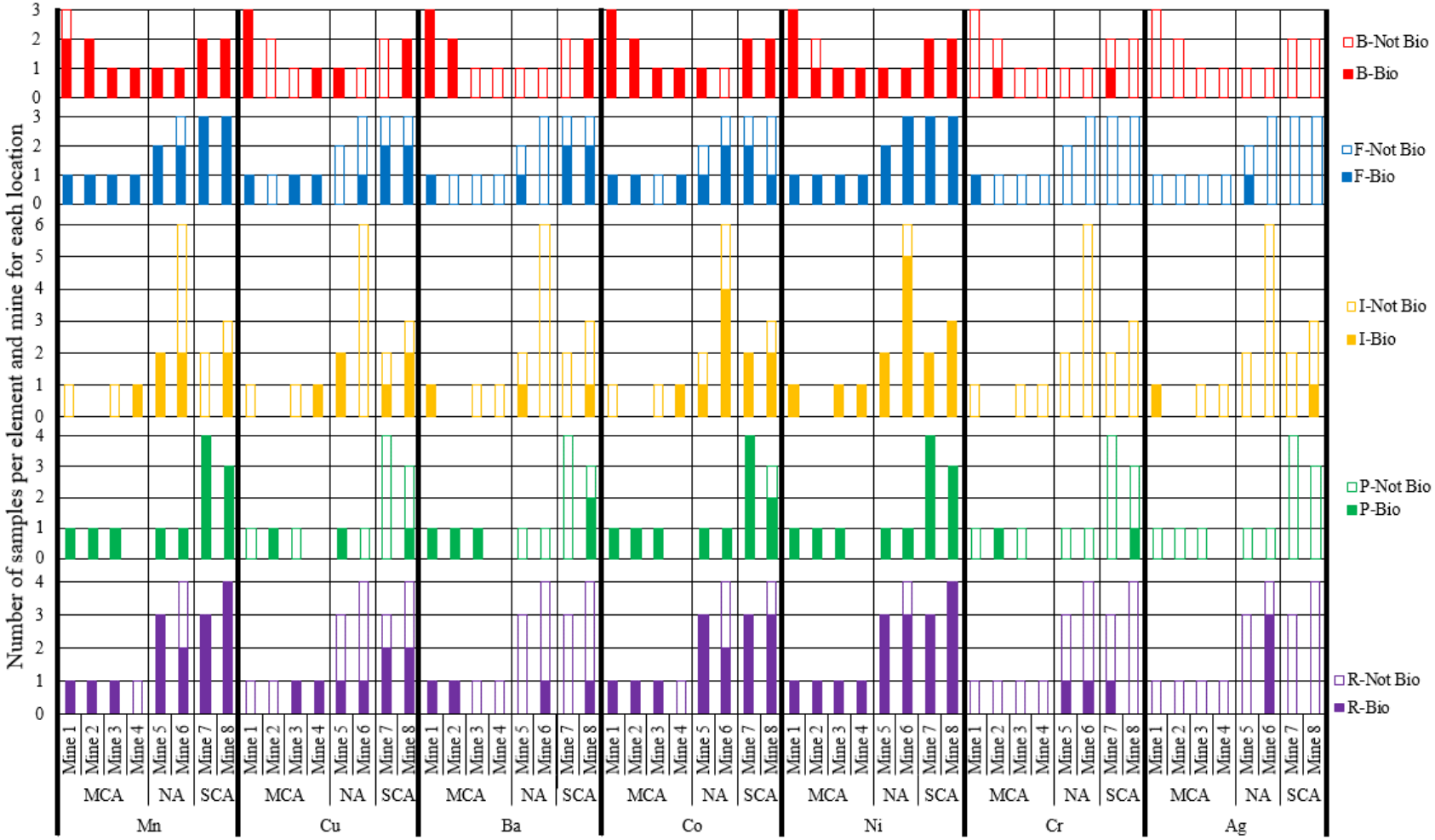

Figure 19. Total number of samples by mine and sampling location (B=roof bolter, F=feeder, I=intake, P=production, R=return), with number of samples having potentially bioaccessible concentrations of common trace elements also identified (i.e., by filled bars). For example, a total of three B samples were analyzed from Mine 1, two of which had potentially bioaccessible Mn concentrations.

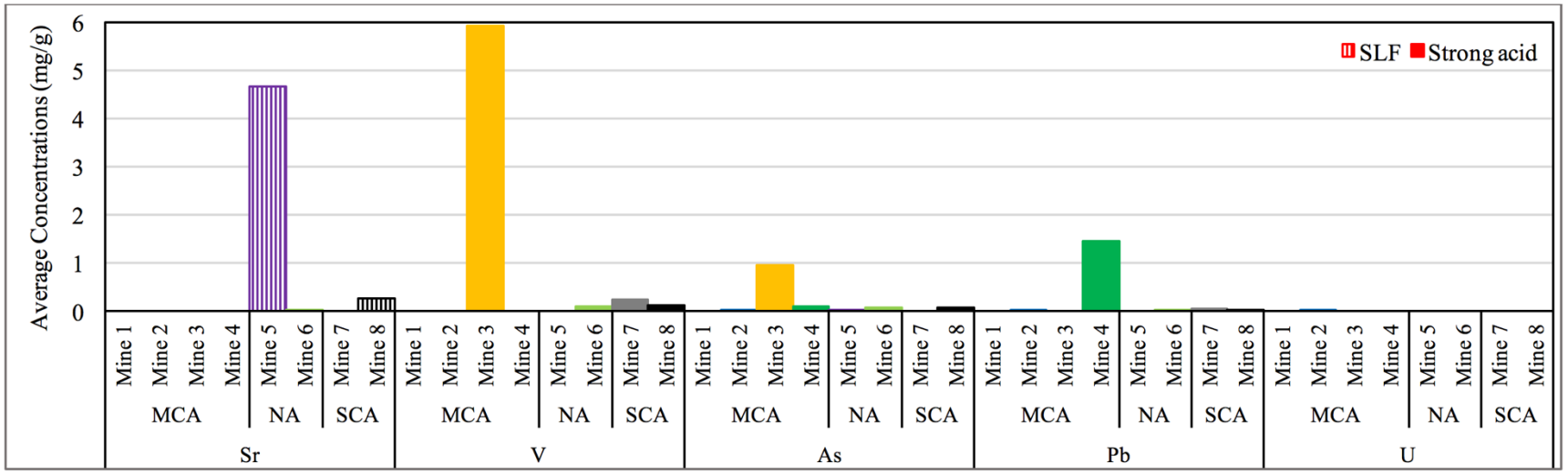

Figure 20. Average concentrations of rare trace elements by mine. The total bar height shows the total acid soluble concentration, and the portion of the bar shown with a vertical pattern shows the potentially bioaccessible concentration (i.e., the portion dissolved in the SLF solution).

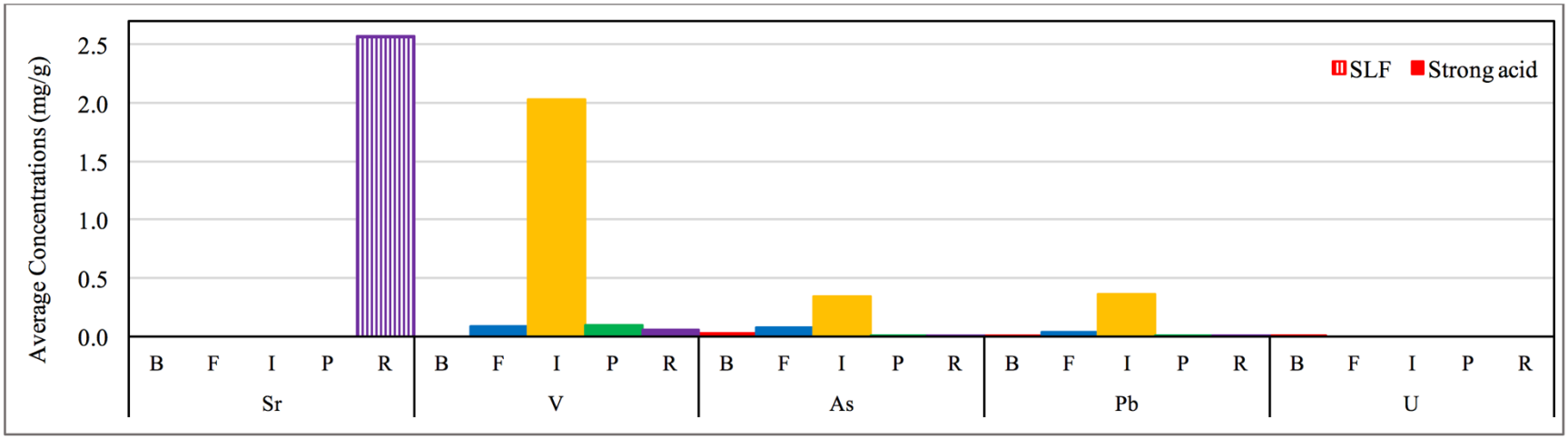

Figure 21. Average concentrations of rare trace elements by sampling location (B=roof bolter, F=feeder, I=intake, P=production, R=return). The total bar height shows the total acid soluble concentration, and the portion of the bar shown with a vertical pattern shows the potentially bioaccessible concentration (i.e., the portion dissolved in the SLF solution).

Appendix D – Additional Results for 1-NP Analysis

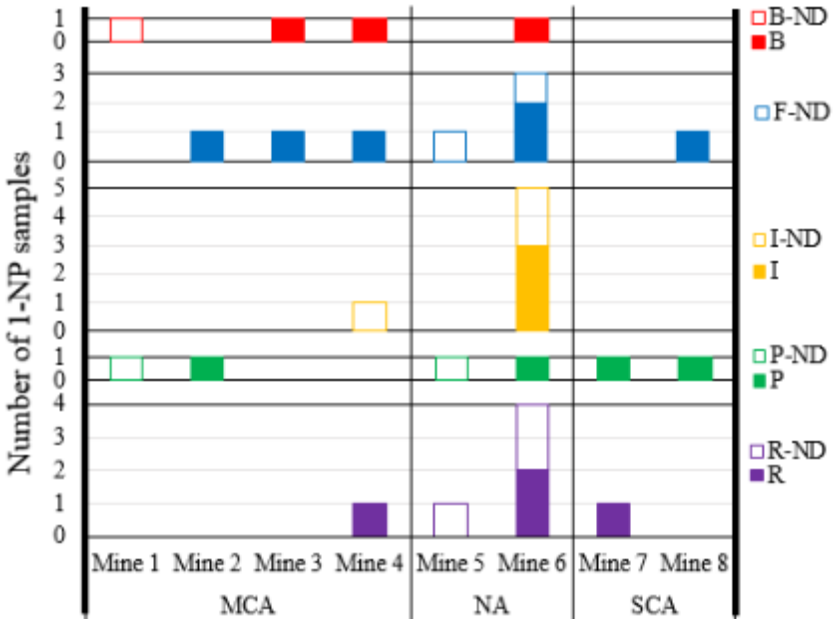

Figure 22. Total number of samples by mine and sampling location (B=roof bolter, F=feeder, I=intake, P=production, R=return), with number of samples having measureable 1-NP also identified (i.e., by filled bars). For example, a total of three F samples were analyzed from Mine 6, two of which had measureable 1-NP.